HIPPOCAMPUS 23:1212–1230 (2013)

Distinct Increased Metabotropic Glutamate Receptor Type 5 (mGluR5) in Temporal Lobe Epilepsy With and Without Hippocampal Sclerosis

Ludmyla Kandratavicius,[1,2] Pedro Rosa-Neto,[3] Mariana Raquel Monteiro,[1] Marie-Christine Guiot,[4] Joao Alberto Assirati Jr,[5] Carlos Gilberto Carlotti Jr,[5] Eliane Kobayashi,[2] and Joao Pereira Leite[1]*

ABSTRACT: Metabotropic glutamate receptor type 5 (mGluR5) upregulation in temporal lobe epilepsy (TLE) and the correlation of its expression with features of hippocampal sclerosis (HS) remains unclear. Here we characterized mGluR5 immunoreactivity in hippocampus, entorhinal cortex (EC), and subiculum of TLE specimens with confirmed HS, with neocortical TLE (non-HS) and necropsy controls. We correlated mGluR5 immunoreactivity with neuronal density, mossy fiber sprouting, astrogliosis (GFAP), and dendritic alterations (MAP2). TLE specimens showed increased mGluR5 expression, which was most pronounced in the EC, subiculum, CA2, and dentate gyrus outer molecular layer. Increased mGluR5 expression was seen in hippocampal head and body segments and was independent of neuronal density, astrogliosis, or dendritic alterations. Positive correlation between mGluR5 expression with mossy fiber sprouting and with MAP2 in CA3 and CA1 was found only in HS specimens. Negative correlation between mGluR5 expression with seizure frequency and epilepsy duration was found only in non-HS cases. Specimens from HS patients without previous history of febrile seizure (FS) showed higher mGluR5 and MAP2 expression in CA2. Our study suggests that mGluR5 upregulation is part of a repertoire of post-synaptic adaptations that might control overexcitation and excessive glutamate release rather than a dysfunction that leads to seizure facilitation. That would explain why non-HS cases, on which seizures are likely to originate outside the hippocampal formation, also exhibit upregulated mGluR5. On the other hand, lower mGluR5 expression was related to increased seizure frequency. In addition to its role in hyperexcitability, mGluR5 upregulation could play a role in counterbalance mechanisms along the hyperexcitable circuitry uniquely altered in sclerotic hippocampal formation. Inefficient post-synaptic compensatory morphological (dendritic branching) and glutamatergic (mGluR5 expression) mechanisms in CA2 subfield could potentially underlie the association of FS with HS and TLE. © 2013 Wiley Periodicals, Inc.

KEY WORDS: hippocampal sclerosis; entorhinal cortex; subiculum; CA2; febrile seizures

[1] **Department of Neurosciences and Behavior, Ribeirao Preto Medical School, University of Sao Paulo, Brazil;** [2] **Department of Neurology and Neurosurgery, Montreal Neurological Institute, McGill University, Montreal, Canada;** [3] **Translational Neuroimaging Laboratory, Department of Neurology and Neurosurgery, Douglas Research Institute, McGill University, Montreal, Canada;** [4] **Department of Pathology, Montreal Neurological Institute, McGill University, Montreal, Canada;** [5] **Department of Surgery, Ribeirao Preto Medical School, University of Sao Paulo, Brazil**

Abbreviations used: CPS, complex partial seizures; DG, dentate gyrus; DG-ML, dentate gyrus molecular layer; EC, entorhinal cortex; EEG, electroencephalography; FS, febrile seizures; GFAP, glial fibrillary acidic protein; GTCS, generalized tonic-clonic seizures; HS, hippocampal sclerosis (belonging to the mesial TLE subtype); IML, inner molecular layer; IPI, initial precipitant injury; IR, immunoreactive; MAP2, microtubule-associated protein 2; mGluR5, metabotropic glutamate receptor type 5; MRI, magnetic resonance imaging; MTLE, mesial temporal lobe epilepsy; NA, not applicable; non-HS, without hippocampal sclerosis (belonging to the neocortical TLE subtype); OML, outer molecular layer; PBS, phosphate buffered saline; SD, standard deviation; TLE, temporal lobe epilepsy.

Grant sponsors: Fundacao de Apoio a Pesquisa do Estado de Sao Paulo – Fapesp (to LK and JPL) and McGill research funds (to EK); Conselho Nacional de Desenvolvimento Cientifico e Tecnologico (CNPq); Grant numbers: Fapesp 07/56721-7 to LK, Fapesp CInAPCe Project 05/56447-7 to JPL.

*Correspondence to: Joao Pereira Leite, Ribeirao Preto Medical School, Department of Neurosciences and Behavior, University of Sao Paulo, Av Bandeirantes 3900, 14049-900, Ribeirao Preto, SP, Brazil. E-mail: jpleite@fmrp.usp.br

Accepted for publication 31 May 2013.
DOI 10.1002/hipo.22160
Published online 23 July 2013 in Wiley Online Library (wileyonlinelibrary.com).

INTRODUCTION

Temporal lobe epilepsy (TLE) is the most common cause of intractable epilepsy and may present with two major forms: the mesial subtype (MTLE) and the extra-temporal, lateral, or neocortical subtype (Mathern et al., 1995a). In MTLE, seizures originate within the mesial aspects of the temporal regions, particularly in the hippocampus (Engel, 2001). Surgical specimens from MTLE patients often display hippocampal sclerosis (HS), which is characterized by neuronal loss, gliosis, fascia dentata mossy fiber sprouting (Babb et al., 1984a; Babb et al., 1991; Mathern et al., 1995a; Kandratavicius et al., 2012), and dendritic abnormalities (Scheibel et al., 1974; Isokawa, 1997). Neocortical TLE (non-HS) shows extra-hippocampal macroscopic mass lesions, such as a low-grade glioma, cortical dysplasia, and hamartoma, and the hippocampus may or may not show some minor cell loss at pathological examination (Mathern et al., 2002).

Previous studies have provided qualitative hippocampal metabotropic glutamate receptor type 5 (mGluR5) analyses of the dentate gyrus (DG) and Ammon's horn (Blumcke et al., 2000; Tang et al., 2001; Notenboom et al., 2006). Immunohistochemistry and western blot have shown hippocampal mGluR5 upregulation in

TABLE 1.

Clinical and Demographic Variables in Epilepsy and Control Groups

Clinical variable	HS (n = 35)	non-HS (n = 7)	Necropsy (n = 8)	P
Age at collection				
Years ± SD	36 ± 7	26 ± 13*	49 ± 18*	***0.01***
Collected side				
Right/left	18/17	4/3	4/4	*0.84*
Gender				
Male/female	17/18	2/5	3/5	*0.45*
Duration of epilepsy				
Years ± SD	25 ± 8*	12 ± 9*	NA	***<0.01***
Frequency of seizures				
#/month ± SD	12 ± 9	36 ± 44	NA	*0.16*
Seizure type				
CPS/CPS+GTCS	10/25	3/4	NA	*0.41*
HS side (based on MRI)				
Right/left/bilateral	16/17/2	NA	NA	–
IPI presence				
Yes/no	21/14*	1/6*	NA	***0.02***
FS in childhood				
yes/no/undetermined	10/16/9	1/6/0	NA	*0.38*

SD, standard deviation; NA, not applicable; CPS, complex partial seizure; GTCS, generalized tonic-clonic seizure; HS, hippocampal sclerosis; MRI, magnetic resonance imaging; IPI, initial precipitant injury; FS, febrile seizure. Bold P-values indicate significant differences between groups, indicated by asterisks. P-values computed by using Student's t-test or Exact Fisher's test.

TLE (Tang et al., 2001; Notenboom et al., 2006), the significance of which is still unclear. In addition, the correlation of mGluR5 upregulation with other classical pathological hallmarks of HS has not yet been described. Important antecedents such as history of febrile seizures (FS) during childhood have not been evaluated in mGluR5 epilepsy literature to date. Such correlations could provide further insights into a possible role of mGluR5 in tissue vulnerability or resilience for developing HS.

Here we characterized mGluR5 expression in subfields of the mesial temporal structures, including the hippocampus, subicular complex, and entorhinal cortex (EC) in a series of TLE specimens on which the hippocampus was the primary site of seizure onset (HS group) (Babb et al., 1984b) and in specimens where the hippocampus is probably secondarily involved (non-HS group). We evaluated whether mGluR5 expression was associated with regional changes of neuronal density, mossy fiber sprouting, MAP2 related-dendritic branching, and astrogliosis. Finally, we investigated differences in mGluR5 expression in specimens from patients with and without history of FS.

PATIENTS AND METHODS

Patients

We analyzed specimens from TLE patients with HS and without HS (freshly collected in the operating room) and non-epileptic controls (from necropsy, collected between 4 and 8 hours after death). A <24-h postmortem time limit allows comparison of necropsy tissue with freshly collected surgical specimens for their protein levels, cell morphology, and tissue integrity (Gittins and Harrison, 2004; Stan et al., 2006), as well as mGluR5 immunoreactivity (Notenboom et al., 2006). Tissue collection and processing were conducted according to the protocol approved by our institution's Research Ethics Board.

Clinical and demographic data of patients and controls are described in Table 1. Non-HS collected hippocampi were from younger patients than non-epileptic necropsy controls but non-HS age at surgery was not different from HS patients. Side collected and gender did not differ among groups. Duration of epilepsy and number of patients with a history of an IPI were higher in the HS group than in non-HS.

HS specimens were derived from 35 MTLE patients (20–50 years old) who underwent a standard en bloc anterior temporal resection (including 3–4 cm of the hippocampus) for medically intractable seizures. All had clinical neuropathological confirmation of HS. According to Blümcke's HS categories (Blumcke et al., 2012), 17 patients had severe HS, 12 classical HS, 3 CA1 HS, and 3 CA4 HS. Non-HS specimens were derived from seven neocortical TLE (8–40 years old) with the following neuropathological diagnostic: two patients had dysembryoplastic neuroepithelial tumor, one leptomeningeal glioneuronal heterotopia, two cortical dysplasia, one cortical dysplasia associated with ganglioglioma, and one diffuse fibrillar astrocytoma. Non-epileptic controls (n = 8) from necropsy were 18–65-years old at death. Underlying diseases

causing death were cardiomyopathy, pulmonary infarct, or renal-hepatic failure, with no history of hypoxic episodes during agony, seizures, or neurological diseases. Furthermore, there was no evidence of brain pathological abnormalities on clinical postmortem examination of the mesial temporal lobe structures.

Clinical Features of TLE Patients

All patients were referred for pre-surgical assessment due to drug-resistant seizures (Berg, 2009). Patients were evaluated at the Ribeirao Preto Epilepsy Surgery Program using standardized protocols approved by the institution's Ethics Committee and a written consent form was obtained from all subjects. Pre-surgical investigation at the Epilepsy Monitoring Unit included detailed clinical history, neurological examination, interictal and ictal scalp/sphenoidal electroencephalography (EEG), neuropsychology evaluation, and intracarotid amobarbital memory and language procedure whenever deemed clinically necessary.

Definition of MTLE (HS group) followed Engel's criteria (Engel, 1996): (1) Seizure semiology consistent with MTLE, usually with epigastric/autonomic/psychic auras, followed by complex partial seizures; (2) pre-surgical investigation confirming seizure onset zone in the temporal lobe; (3) anterior and mesial temporal interictal spikes on EEG; (3) no lesions other than uni- or bilateral hippocampal atrophy on high-resolution magnetic resonance imaging scans (reduced hippocampal dimensions and increased T2 signal); (4) clinical histopathological examination compatible with HS; (5) no evidence of dual pathology identifiable by any of the assessment methods described (clinical, electrophysiology, neuroimaging, and histopathology).

Information regarding antecedent of FS, seizure types, and estimated monthly frequency (within the two years prior to surgery) were retrospectively collected from medical records for each patient.

Exclusion criteria in HS group were: (1) focal neurological abnormalities on physical examination, (2) generalized or extra-temporal EEG spikes, (3) marked cognitive impairment indicating dysfunction beyond the temporal regions, and (4) history of previous psychiatric disorders or substance dependence.

Tissue Collection and Immunohistochemical Processing

Specimens from hippocampal head ($n = 14$ HS; $n = 1$ non-HS; $n = 2$ controls) and body ($n = 21$ HS; $n = 6$ non-HS; $n = 6$ controls) were segmented into 1-cm blocks transversely oriented to the hippocampal long axis. Blocks were placed in neo-Timm's fixative solution [0.1% sodium sulfide (Sigma, St Louis, USA) in Millonig's buffered glutaraldehyde (Vetec, Rio de Janeiro, Brazil)] or buffered paraformaldehyde (Sigma, St Louis, USA). After 48–96 hours, specimens were processed for neo-Timm histochemistry and hematoxylin-eosin (Laborclin, Pinhais, Brazil) staining, or paraffin embedded for immunohistochemistry.

For neo-Timm staining (Babb et al., 1991), cryostat sections were mounted on chrome-alum gelatin-coated slides and air dried. Slides were processed in batches containing at least one HS and two controls slides. Slides were immersed in a physical developer maintained at 26°C in a darkroom. Developer consisted of 10 mL of a 50% gum arabic (Sigma, St Louis, USA) solution, 30 mL of an aqueous solution of 1.3*M* citric acid (Merck, Darmstadt, Germany), 0.9*M* sodium citrate (Merck, Darmstadt, Germany), 90 mL of an aqueous solution of 0.5*M* hydroquinone (Merck, Darmstadt, Germany), and 1.5 mL of a 17% silver nitrate solution (Merck, Darmstadt, Germany). Light sections were developed for 40 min and dark sections for 50 min. Slides were washed in distilled water for 5 min and running tap water for 10 min. They were subsequently air-dried, ethanol dehydrated, xylene-cleared, and cover slipped.

Immunohistochemistry was performed with antibodies that identified immunoreactivity for: (1) Neu-N, a nuclear protein found in the nuclei of mature neurons (1:1000 dilution; Chemicon, Temecula, USA); (2) glial fibrillary acidic protein (GFAP), an intracytoplasmic filamentous protein constituent of astrocytes cytoskeleton (6F2, 1:500 dilution; Dako, Glostrup, Denmark); (3) microtubule-associated protein 2 (MAP2), a protein found in perycaria and dendrites of mature neurons (H-300, 1:200 dilution; Santa Cruz Biotechnology, Santa Cruz, USA); and (4) mGluR5 (ab5675, 1:100 dilution; Millipore, Billerica, USA); this antibody shows no cross-reactivity with mGluR1 according to the manufacturer and this has been specifically verified in Notenboom et al. (2006). Briefly, paraffin embedded HS, non-HS, and control hippocampi were processed together as described in Kandratavicius et al. (2012) and developed simultaneously for 10 min in 0.05% 3,3′-diaminobenzidine tetrahydrochloride (Pierce, Rockford, USA) and 0.01% hydrogen peroxide (Merck, Darmstadt, Germany). After sufficient colorization, reaction was halted by washing in several rinses of distilled water, dehydrated through graded ethanol to xylene (Merck, Darmstadt, Germany), and cover slipped with Krystalon (EM Science, Gibbstown, USA). Adjacent sections were hematoxilin-eosin stained and examined for tissue integrity. Control sections without the primary antisera did not reveal staining (data not shown).

Immunofluorescence and Confocal Microscopy

Sections were submitted to the same procedures as described above except that overnight incubation was performed with a mix of mGluR5 + GFAP (1:100). After phosphate buffered saline (PBS) pH 7.4 washing, sections were incubated for 2 hours in secondary Texas Red antibodies (T862, anti-mouse, Molecular Probes, Eugene, USA) used in combination with Alexa Fluor 488 (A11008, anti-rabbit, Molecular Probes, Eugene, USA), diluted at 1:200 in PBS. From this step, all procedures were done shielded from light to prevent possible bleaching. After PBS washing, sections were incubated with Hoechst solution (4 μg/mL, Molecular Probes, Eugene, USA) for 4 min. After PBS washing, sections were mounted on Fluoromount-G (Electron Microscopy Sciences, Fort Washington, USA), sealed, and dried overnight. Fluorescent-stained sections were visualized with a Leica TCS-SP5 AOBS confocal laser microscope (Leica Microsystems, Heidelberg, Germany). Images were analyzed with 20× and 63× oil immersion lenses,

and digital images were acquired and processed by the imaging software LAS-AF (version 2.1.0).

Cell Count, Astrogliosis, and Neo-Timm Quantification

HS, non-HS, and control hippocampi were compared for neuronal density, neo-Timm's staining, and GFAP expression. Neuronal counting was performed based on Lorente de No's classification (Lorente de No, 1934), including fascia dentata granular and subgranular cells, hilar neurons, as well as pyramidal cells in CA4, CA3, CA2, CA1, prosubiculum, subiculum, parasubiculum, and EC layer III. Cell densities (neurons per cubic millimeter) were estimated in 8-μm Neu-N stained slices at 400× magnification with a morphometric grid methodology using Abercrombie's correction (Abercrombie, 1946) as previously described (Babb et al., 1984a; Mathern et al., 1995a; Kandratavicius et al., 2012). Astrogliosis was determined by GFAP immunoreactive (IR) area of stained astrocytes and astrocytic fibers in each subfield (see details on quantification method below).

Mossy fiber sprouting was evaluated in neo-Timm stained sections in the hilus, granular layer, and inner molecular layer (IML), always in the superior blade of the DG. Each subfield of each specimen had three different samples measured and averaged for statistical analysis. Measurements of gray value were estimated using Image J analysis system (NIH, USA, public domain). Images were collected and digitized with a high resolution CCD monochrome camera attached to an Olympus microscope. This method was used to obtain digitized images of neo-Timm, Neu-N, GFAP, and MAP2 stained slides. Uniform luminance was maintained and checked every 10 measurements using an optical density standard and a gray value scale ranging from 0 (white) to 255 (black).

Semi-Quantitative Analysis of Immunohistochemistry

Adjacent slides to those examined for neuronal density and astrogliosis were analyzed for MAP2 and mGluR5. Aperio ScanScope (Aperio Technologies, Vista, CA, USA) was used to obtain digitized images of mGluR5 slides. Representative samples of each subfield for mGluR5 quantification were obtained with Image Scope at 10× magnification. In brief, all digitized images were obtained under the same luminance and were further analyzed with Image J software, following the same criteria for other immunohistochemistries: (1) the software identifies the gray value distribution of a subfield's digital image; (2) immunopositive stained area is selected, limited to a fixed threshold range; and (3) threshold range is pre-settled based on control group sections, to exclude the low intensity gray value of background staining from the analysis. A similar approach was used by our group elsewhere (Peixoto-Santos et al., 2012). Results for granular layer included granular cell layer and dentate gyrus molecular layer (DG-ML). Gray values measurements of mGluR5-stained IML and outer molecular layer (OML) were performed as per neo-Timm's staining. Analyses were conducted by one investigator (L.K.), blind to hippocampal pathology and group classification.

Data Analysis

Data were analyzed using the statistical program PAWS (version 18.0) and SigmaPlot (version 11.0). Groups were compared using analysis of variance (ANOVA one way, with Bonferroni post hoc test) or unpaired t test for variables with normal distribution, and Kruskal-Wallis One Way Analysis of Variance on Ranks (with Dunn post hoc test) or Mann-Whitney Rank Sum Test for variables without normal distribution. Fisher Exact test was applied for comparison of relative frequencies of clinical variables between groups. Other statistical tests included analysis of covariance (ANCOVA) and Pearson correlation analyses. Statistical significance was set at $P < 0.05$ and values presented as mean ± SD.

RESULTS

Characterization of HS and Non-HS Hippocampi

Neuronal loss in HS hippocampi varied 32–73% as compared with controls (Fig. 1A, asterisks). HS hippocampi exhibited lower neuronal density than non-HS in the granular layer, CA1, and prosubiculum (Fig. 1A, hash signs). Non-HS hippocampi did not differ from controls in all hippocampal formation subfields. Increased GFAP expression was observed in CA1, prosubiculum, EC, subiculum, and parasubiculum of HS hippocampi, and the latter two subfields also in non-HS specimens (Fig. 1B, asterisks). GFAP IR area was higher in HS than in non-HS (Fig. 1B, hash sign). There was a trend of increased astrogliosis in the granular layer ($P = 0.06$) and CA3 ($P = 0.05$) in the HS group. Aberrant sprouted mossy fibers in the granular layer and IML were seen in HS hippocampi (Fig. 2) and an inverse correlation between IML mossy fiber sprouting and hilar neuronal density was seen ($R = -0.46$; $P = 0.04$).

MAP2 immunohistochemistry (Fig. 3A) showed increased IR area in HS granular layer and CA2. Enhanced staining in HS granular layer comprised both dendritic and cytoplasmatic compartments (compare Fig. 3B–D). Reduced MAP2 expression was seen in HS CA1 and prosubiculum. MAP2 IR area correlated positively with neuronal density in CA4 of controls ($R = +0.78$; $P = 0.02$). In HS hippocampi, we found a negative correlation between MAP2 and neuronal density in CA1 ($R = -0.49$; $P = 0.01$), suggesting that the few surviving neurons in CA1 might exhibit some degree of dendritic sprouting. In Figure 3E, profuse and abnormal dendritic ramification can be seen in HS CA1. In non-HS CA1 (Fig. 3F), MAP2 staining was evident in long and organized dendritic fibers, while in controls (Fig. 3G) dendrites and cell bodies displayed similar immunoreactivity.

mGluR5 Distribution and Quantification

Strong mGluR5 immunostaining was observed in HS and non-HS as compared to controls (Fig. 4A–F). There was no difference in mGluR5 staining pattern and quantification of IR

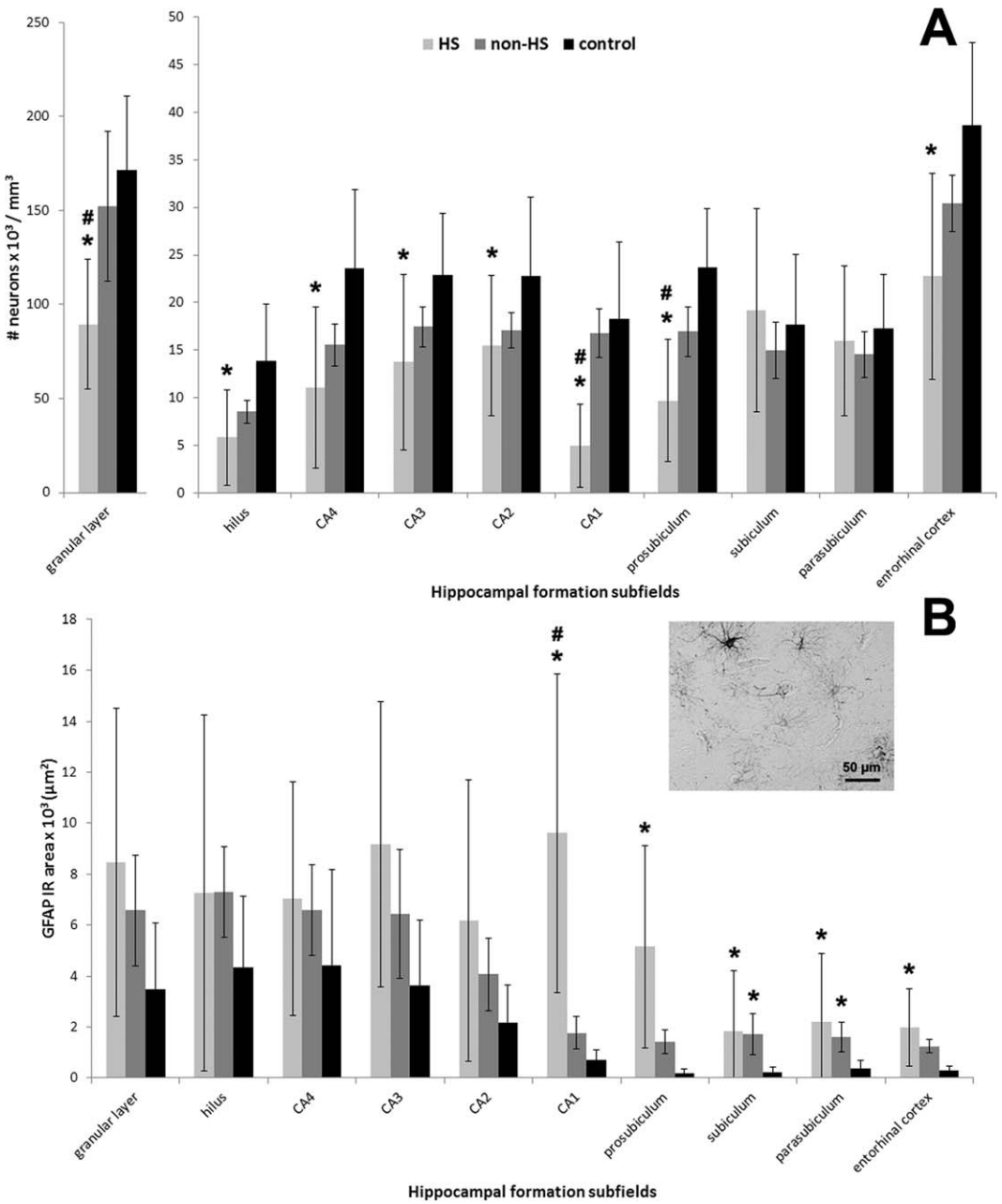

FIGURE 1. Neuronal density and GFAP expression in human hippocampal formation subfields. Neuronal density and GFAP IR area values from HS (light gray bars), non-HS (gray bars), and non-epileptic controls (black bars) are indicated as mean ± std. deviation. Asterisk indicate significant statistical difference ($P < 0.05$) between epileptic and control group. Hash sign indicate significant statistical difference ($P < 0.05$) between epileptic groups. (A) Neuronal loss (based on Neu-N positive cell count) in HS hippocampi was identified in the dentate gyrus (granular layer and hilus), Ammon's horn subfields (CA1-CA4) and prosubiculum when compared to controls. The pattern of neuronal loss followed classical HS description: maximum reduction in CA1 (73%) but also severe (41–59%) in granular layer/hilus/CA4/prosubiculum/entorhinal cortex, with relative preservation of CA2 and CA3 (32–40%). Neuronal density in the subiculum and parasubiculum was similar between the groups. HS granular layer, CA1, and prosubiculum exhibited lower neuronal density than non-HS (hash signs). (B) GFAP IR area measured in the HS hippocampal formation showed increased expression from CA1 to entorhinal cortex when compared to the other groups. In HS CA1, GFAP-IR area was higher than in non-HS. Non-HS hippocampal formation showed astrogliosis in subiculum and parasubiculum as compared to controls. Excerpt on the right illustrates the GFAP-IR pattern seen in HS entorhinal cortex, with ramificated astrocytes and negative stained neuronal nuclei.

area at the level of hippocampal head (i.e., with clear identification of presubiculum islands; Fig. 4A–C) and hippocampal body (Fig. 4D–F) within each group.

a. Dentate gyrus

a1. Molecular layers (Fig. 4G): Gray value measures of mGluR5 staining showed increased immunoreactivity for HS

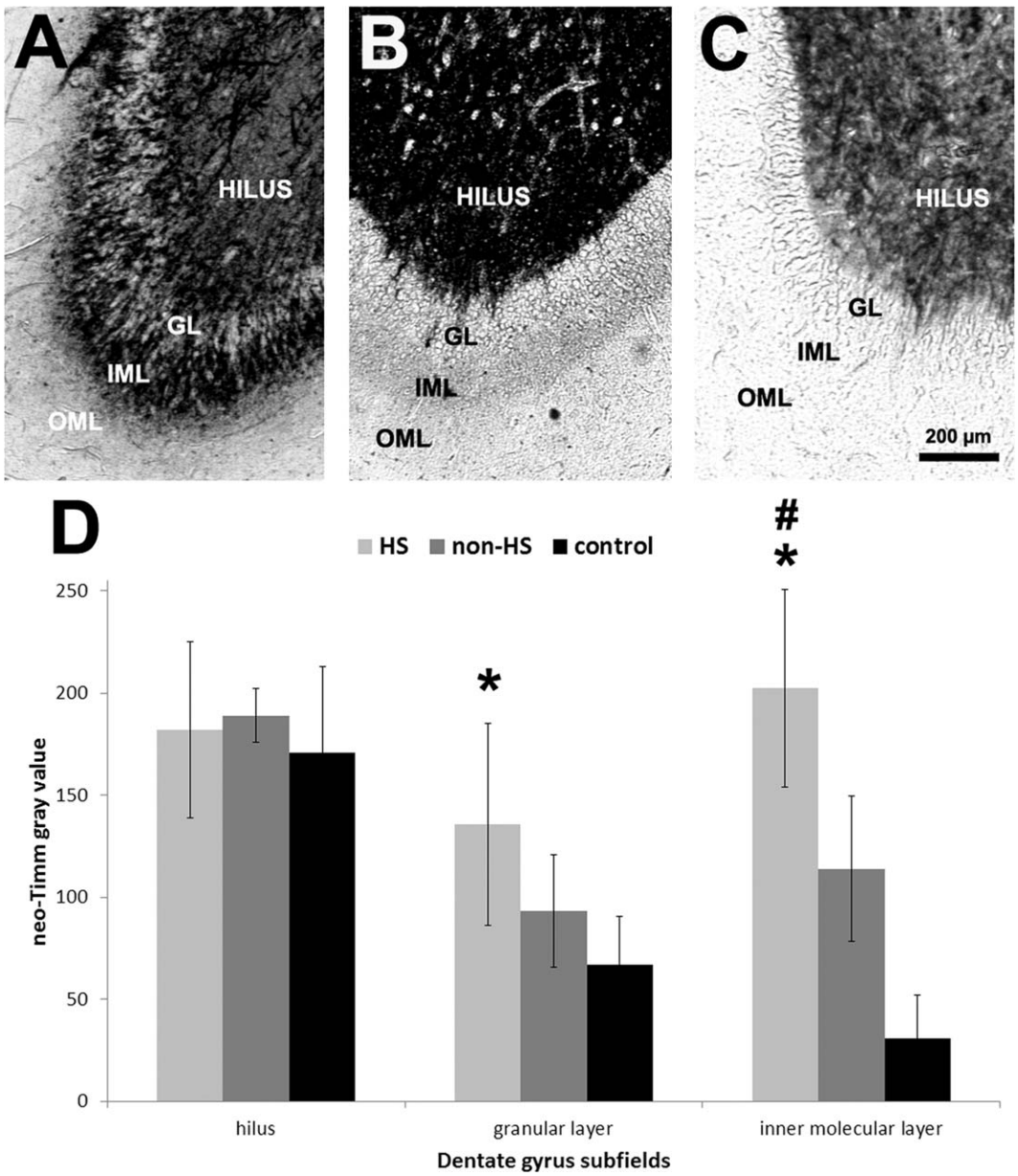

FIGURE 2. Neo-Timm histochemistry of the human dentate gyrus. Low magnification images of neo-Timm stained DG revealed the typical pattern with dark stained hilus in HS (A, light gray bars), non-HS (B, gray bars), and controls (C, black bars) with increased mossy fiber sprouting in HS GL and IML. Gray values in the HS GL were higher than in controls and in the IML were higher in HS group when compared to non-HS and controls. Values indicated as mean ± std. deviation. Asterisk indicate significant statistical difference ($P < 0.05$) between epileptic and control group. Hash sign indicate significant statistical difference ($P < 0.05$) between epileptic groups. OML: outer molecular layer; IML: inner molecular layer; GL: granular layer.

and non-HS in the OML when compared to controls (HS: 74 ± 21; non-HS: 68 ± 11; controls: 43 ± 12; $P < 0.03$) but not in the IML (HS: 58 ± 18; non-HS: 60 ± 9; controls: 50 ± 18; $P = 0.38$). Correlation analysis showed that only in the HS group, the greater OML mGluR5 staining, the greater IML Timm's sprouting values (Fig. 5A; R= +0.51, $P = 0.02$). By contrast, IML mGluR5 staining exhibited a negative correlation with CA4 GFAP in controls (Fig. 5B; $R = -0.79$, $P = 0.02$), but strongly positive in non-HS cases (Fig. 5B; $R = +0.98$, $P = 0.003$).

a2. Hilus: In HS, we found distinctive mGluR5 IR staining in remaining cell bodies and dendrites (Fig. 4H *left*, *arrows*). Although non-HS hilus displayed increased mGluR5 IR area when compared to HS and controls (Fig. 6A), staining pattern in non-HS was more diffuse than in MTLE cases. HS showed also mGluR5-stained fibers of neuronal and likely glial origin, including cells with astrocytic profile near the granular layer border (Fig. 4F *right*, *arrowheads*), which were not evident in non-HS or control hilus. In non-HS group, hilar mGluR5 showed inverse correlation with age (Fig. 5C; $R = -0.82$, P

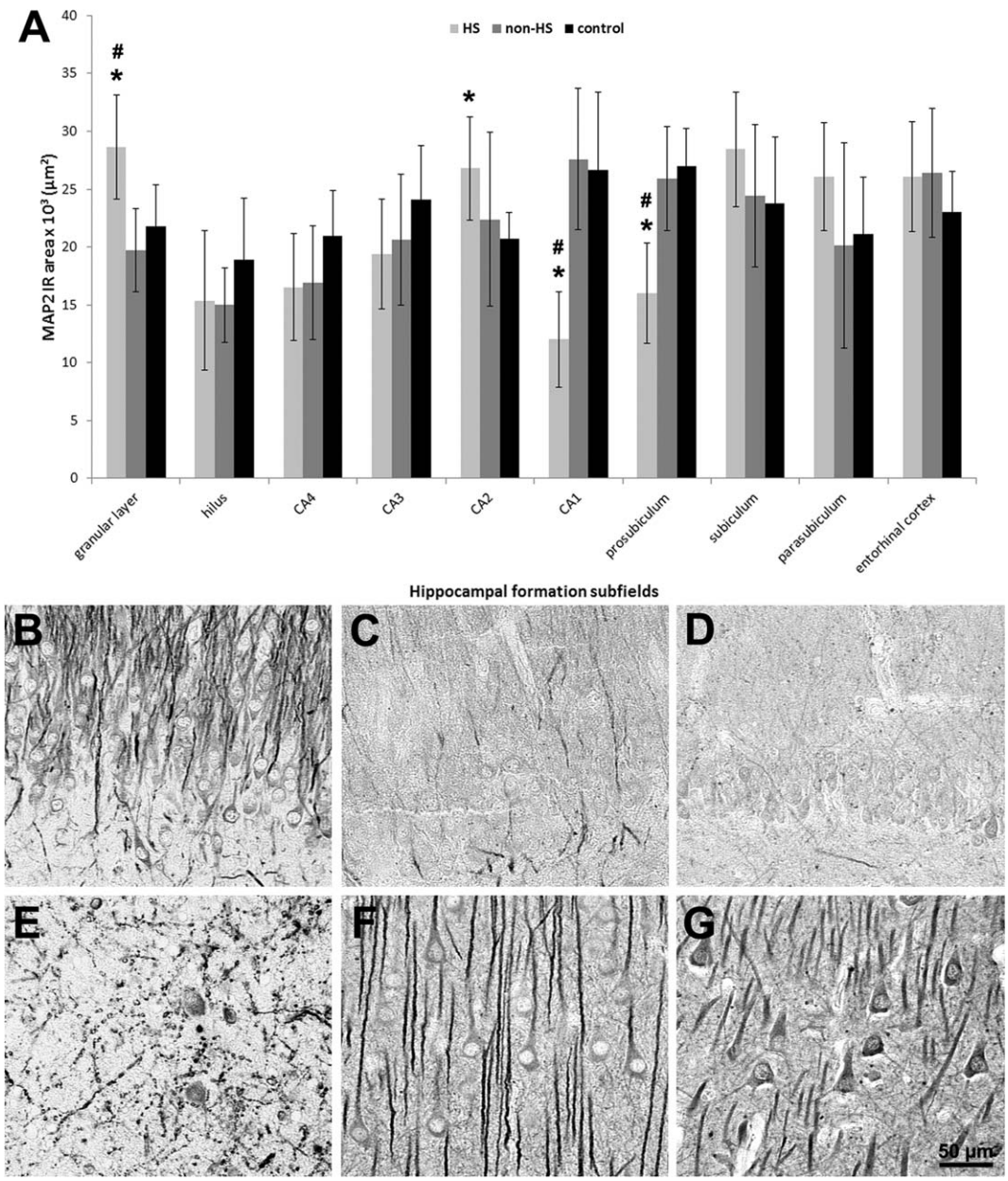

FIGURE 3. MAP2 immunohistochemical expression in human hippocampal formation. (A) Quantification of MAP2 IR area in hippocampal formation subfields of HS (light gray bars), non-HS (gray bars), and control group (black bars). MAP2 expression was increased in the granular layer and CA2 of HS and decreased in CA1 and prosubiculum as compared to controls. HS granular layer, CA1, and prosubiculum also differed from non-HS cases. Values indicated as mean ± std. deviation. Asterisk indicate significant statistical difference ($P < 0.05$) between epileptic and control group. Hash sign indicate significant statistical difference ($P < 0.05$) between epileptic groups. (B–D) In HS granular layer (B), increased MAP2 IR was conspicuous in dendrites and cytoplasm of granular cells, as compared to non-HS (C) and control (D). (E-G) In HS CA1 (E), MAP2 positive staining was seen in abnormally shaped neurons and dendrites, in contrast to the elongated fiber pattern of pyramidal cells in non-HS (F) and control (G).

= 0.02), although age at surgery was not statistically significant different from HS group (see Table 1).

b. Ammon's horn

b1. CA4 (Fig. 7A): Pyramidal neurons of HS hippocampi exhibited increased immunoreactivity (Fig. 7A, left) when compared to the pale neuropil and cell body staining found in controls (Fig. 7A, right). Neuronal density and mGluR5 expression in HS CA4 exhibited positive correlation (Fig. 5D, $R = +0.48$, $P = 0.03$). In non-HS cases, global mGluR5 staining was increased when compared to HS and controls (Fig. 6A), but when mGluR5 IR area was corrected for neuronal density, both epileptic groups were equally upregulated (Fig. 6B).

b2. CA3 and CA2 (Fig. 7B–C): Immunoreactivity in HS CA3 was less pronounced than in CA2, with heterogeneous

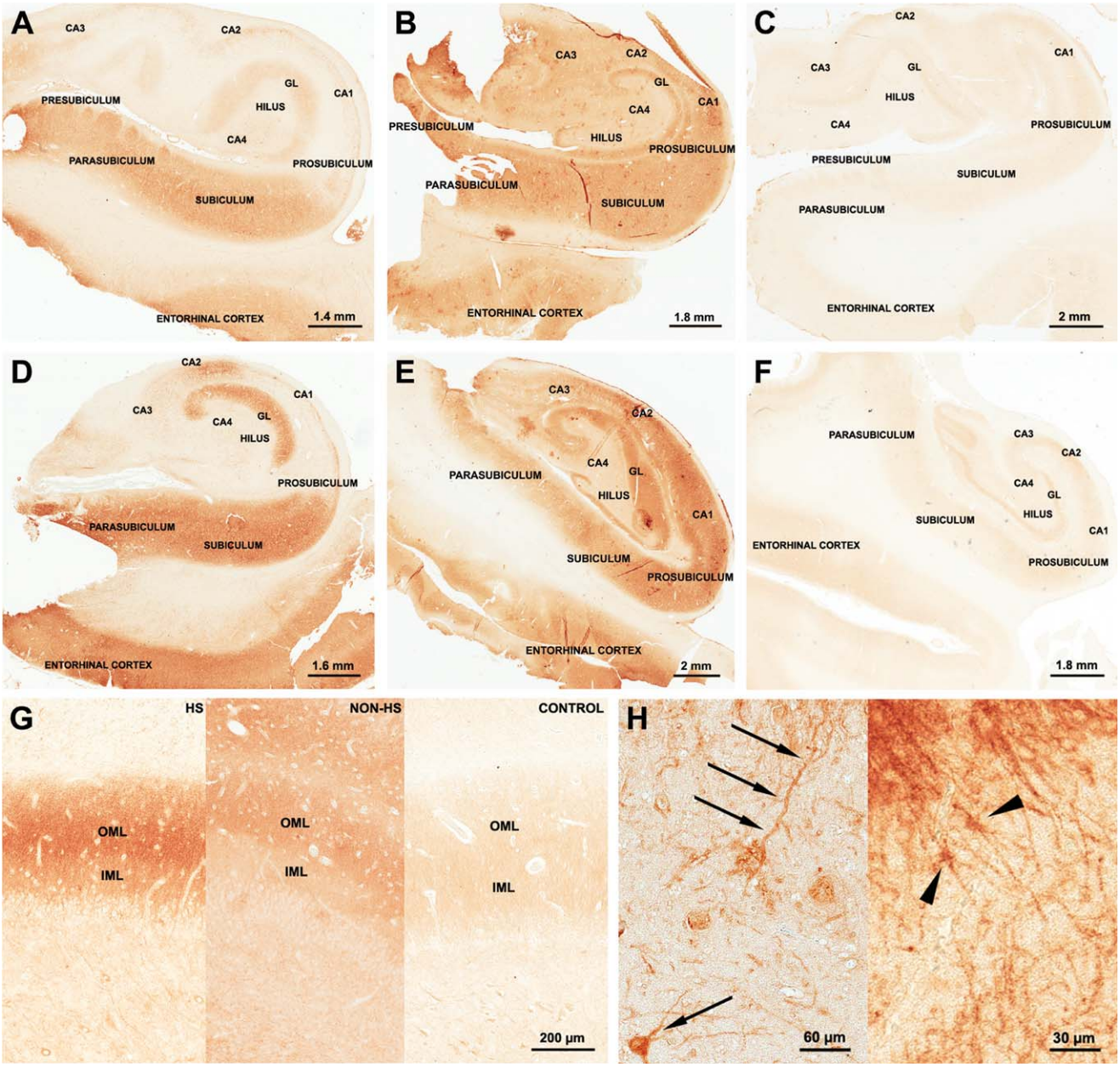

FIGURE 4. mGluR5 immunohistochemical expression in human hippocampal formation: dentate gyrus. Representative mGluR5 staining patterns in HS (A: hippocampal head; D: hippocampal body), non-HS (B: hippocampal head; E: hippocampal body) and control group (C: hippocampal head; F: hippocampal body). HS and non-HS hippocampal head and body showed strong immunostaining when compared to controls. HS and non-HS dentate gyrus OML presented an enhancement of mGluR5 immunoreactivity in relation to IML (G). Such feature was not evident in control dentate gyrus (G, right). Strong mGluR5 staining was also found in postsynaptic terminals as primary dendrites in the hilus (H left, arrows) and in astrocytic-like cells in the dentate gyrus (H right, arrow heads). GL, granular layer; OML, outer molecular layer; IML, inner molecular layer. [Color figure can be viewed in the online issue, which is available at wileyonlinelibrary.com.]

staining of remaining pyramidal neurons and dendrites (Fig. 7B). HS CA2 displayed a rather distinct staining pattern, with strong mGluR5 labeling in stratum pyramidale and radiatum-lacunosum. mGluR5 immunoreactivity was also increased in CA2 interneurons (Fig. 7C, left, arrowheads). In non-HS CA3 and CA2, a dense neuropil staining was seen, as well as in dendrites, and less pronounced in cell bodies (Fig. 7C, right). In controls, CA2 and CA3 staining patterns were similar to that in CA4. mGluR5 IR area quantification in CA3 and CA2 was higher in HS and non-HS groups as compared to controls, and increased in non-HS when compared to HS (Fig. 6A). Corrected by neuronal density (Fig. 6B) mGluR5 IR staining was still higher in CA2 non-HS than in HS. Interneurons at the pyramidale-oriens margin were strongly

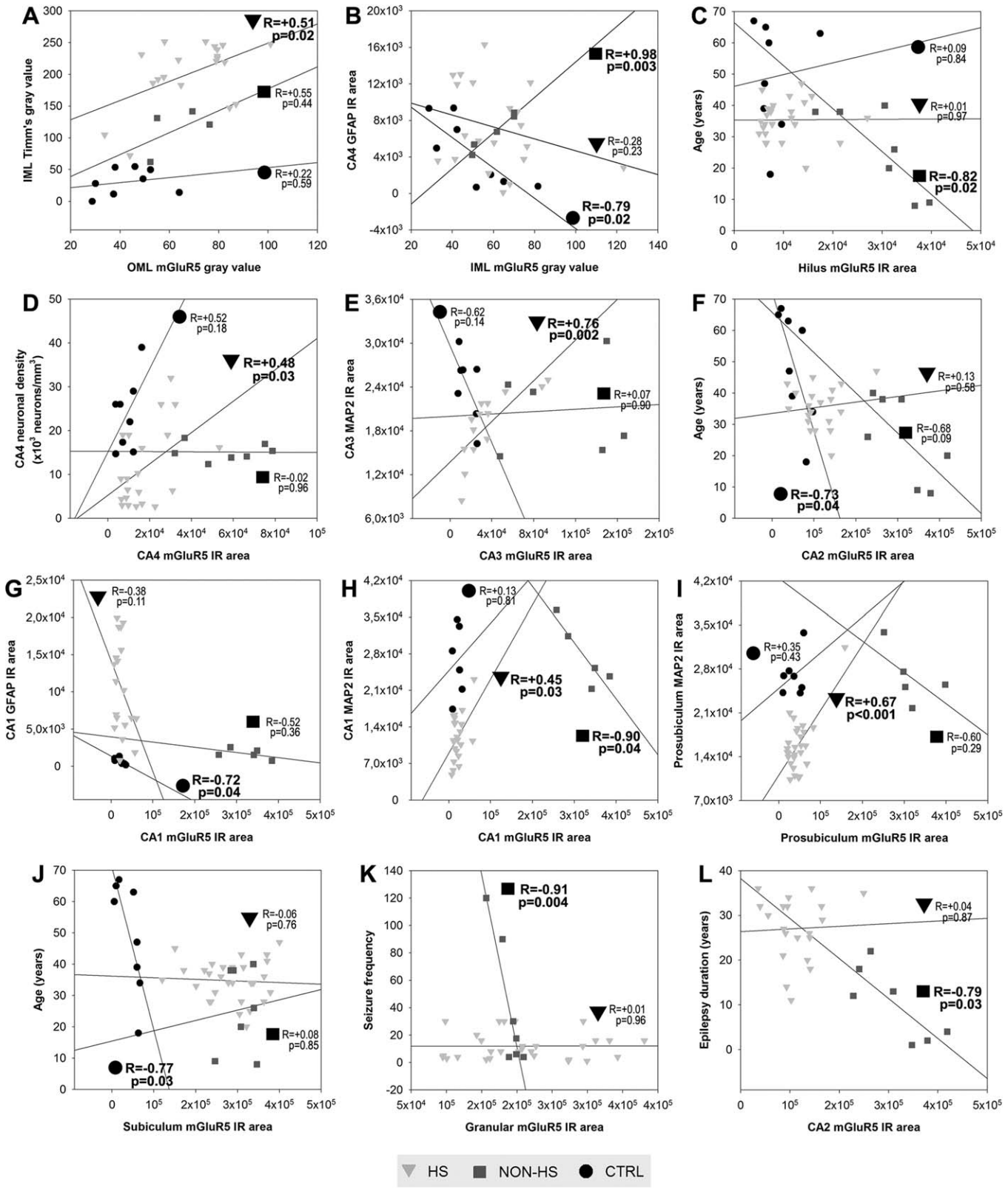

FIGURE 5. Correlation of clinical and neuropathological data with mGluR5 expression in human hippocampal formation. Triangles represent HS data; squares represent non-HS data; circles represent control data. Statistically significant correlations are indicated as boldfaced values on each graphic.

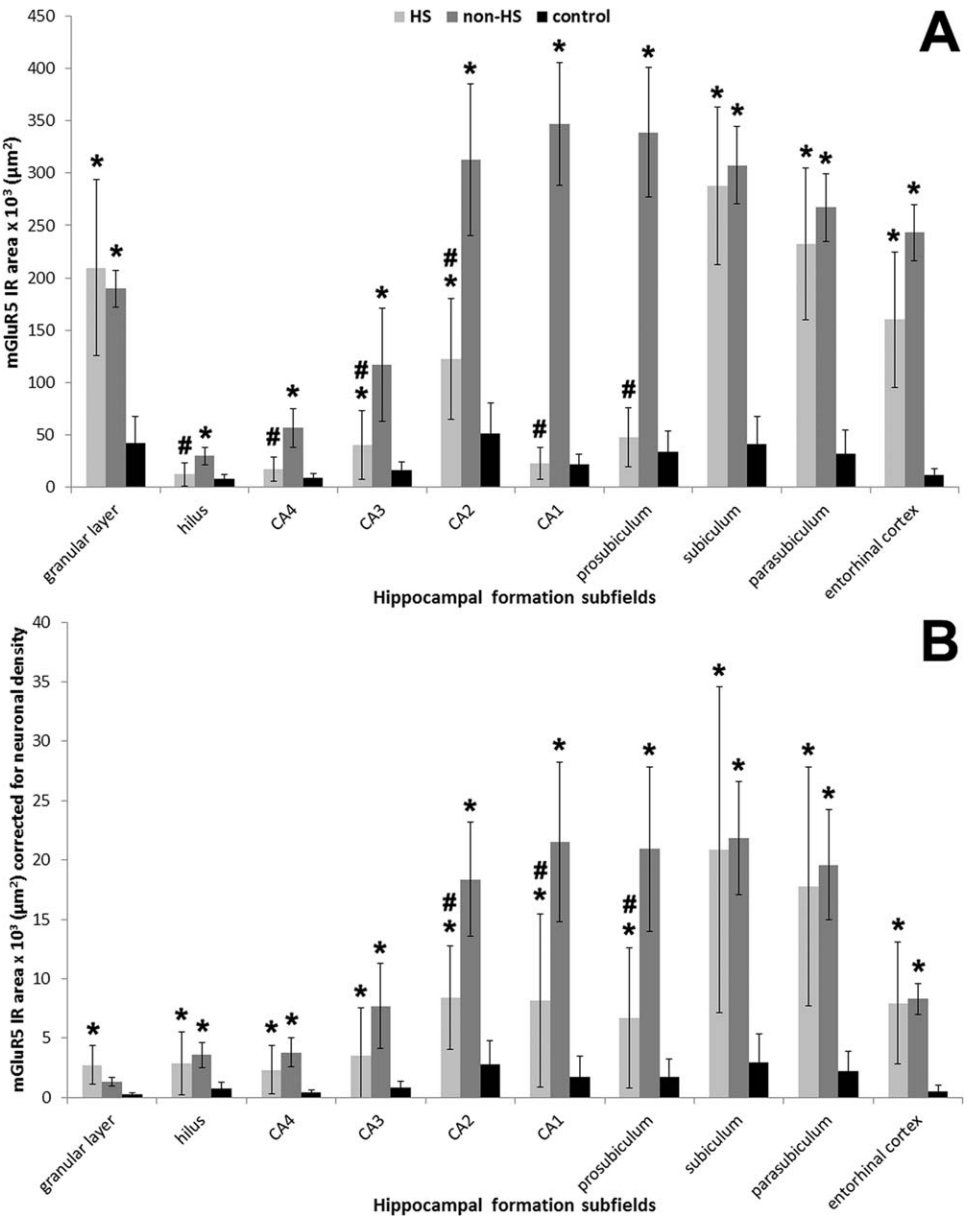

FIGURE 6. mGluR5 quantification in different subfields of the hippocampal formation. (A) mGluR5 expression without neuronal density correction revealed increased IR area in all subfields of non-HS (gray bars) as compared to controls (black bars). HS (light gray bars) mGluR5 expression in the hilus, CA1–4, and prosubiculum were lower than in non-HS. (B) mGluR5 IR area levels per neuron (i.e., corrected for neuron densities) showed upregulation in all hippocampal formation subfields of HS and non-HS cases when compared to controls. CA2, CA1, and prosubiculum mGluR5 levels per neuron in HS cases were lower than in non-HS cases. Values indicated as mean ± std. deviation. Asterisk indicate significant statistical difference ($P < 0.05$) between epileptic and control group. Hash sign indicate significant statistical difference ($P < 0.05$) between epileptic groups.

stained in HS (Fig. 7D, left, arrow), but not in non-HS cases (Fig. 7D, right). In HS group, CA3 MAP2 and mGluR5 expression exhibited a strong positive correlation (Fig. 5E, $R = +0.76$, $P = 0.002$), suggesting a mGluR5 dendritic sprouting that occurs only in MTLE. In CA2, mGluR5 IR area inversely correlated with age in controls (Fig. 5F, $R = -0.73$, $P = 0.04$).

b3. Sommer's sector (Fig. 7E,F): Surviving neurons in CA1 (Fig. 7E, left) and prosubiculum (Fig. 7F) of HS hippocampi exhibited strong cytoplasmic mGluR5 staining and massive entanglement of mGluR5 positive fibers within the stratum pyramidale. Non-HS cases showed strong neuropil and dendritic staining (Fig. 7E, right). In contrast, pyramidal cells in control specimens showed light immunoreactivity, with a widespread pale neuropil staining. mGluR5 quantification showed no difference between HS and controls (Fig. 6A), but mGluR5 IR area corrected by neuronal density was higher in both Sommer's sector subfields in HS (Fig. 6B).

Non-HS hippocampi exhibited increased immunoreactivity as compared to HS and controls (Fig. 6A,B). CA1 mGluR5 IR area showed inverse correlation with CA1 GFAP in controls (Fig. 5G, $R = -0.72$, $P = 0.04$) and inverse correlation with CA1 MAP2 in non-HS (Fig. 5H, $R = -0.90$, $P = 0.04$). However, in HS hippocampi, CA1 mGluR5 IR area showed

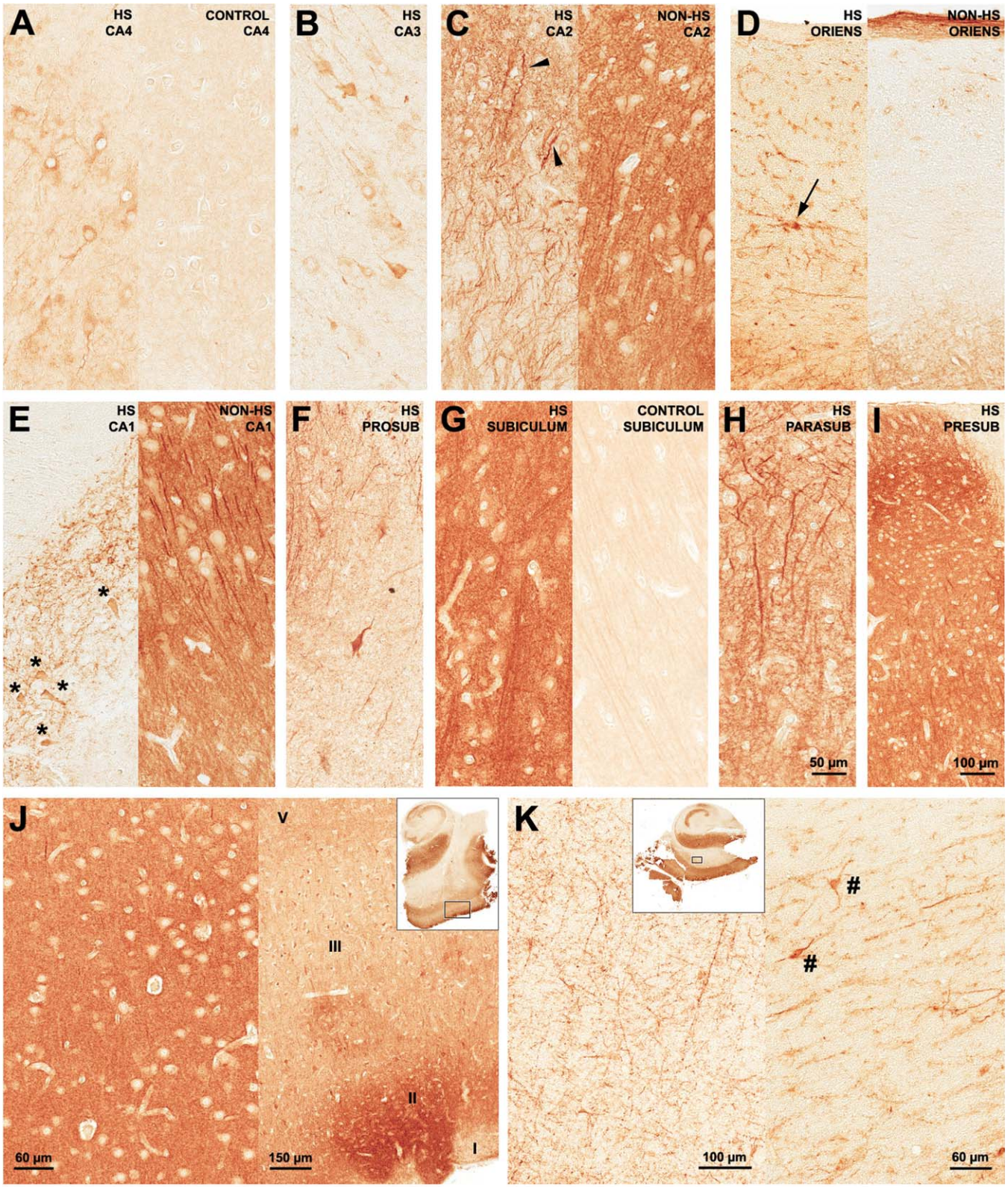

FIGURE 7.

positive correlation with CA1 MAP2 (Fig. 5H, $R = +0.45$, $P = 0.03$), similar to what was seen in HS CA3. The same occurred in HS prosubiculum, also suggestive of mGluR5 dendritic sprouting (Fig. 5I, $R = +0.67$, $P < 0.001$).

c. Subicular complex: Pronounced staining of long dendritic processes in HS subiculum was observed, with dense mGluR5 immunoreactivity in neuropil and neuronal cell bodies (Fig. 7G, left). In controls, pyramidal cell bodies and long dendritic fibers showed evident mGluR5 IR, although much less pronounced than in HS (Fig. 7G, right). Nuclei and blood vessels were devoid of mGluR5 IR. In addition, there was evident apical dendritic staining in the parasubiculum of epileptic cases (Fig. 7H). Neuronal clusters from presubiculum also showed strong staining in neuropil and cell bodies (Fig. 7I). In the subiculum/parasubiculum, mGluR5 IR area was 6.9–8.4-fold higher in epileptic groups than in controls (Fig. 6A). Similar to what was found in control CA2, control subiculum exhibited inverse correlation with age (Fig. 5J, $R = -0.77$, $P = 0.03$).

d. Entorhinal cortex: HS neuropil was intensely stained, most often stronger than in cell bodies of layer III pyramidal cells (Fig. 7J, left). mGluR5 immunoreactivity was also intense in layer II islands (Fig. 7J, right), which give rise to the perforant path projections that reach granular cells. Other cell layers also exhibited strong labeling (Fig. 7J, right). Staining pattern in HS and non-HS was similar in HS and non-HS cases, although stronger in the latter. Quantification of IR area identified the EC as the subfield with the strongest mGluR5 staining in the whole hippocampal formation (Fig. 6A). Indeed, HS EC showed 14-fold and non-HS 21-fold more mGluR5 IR area than control specimens. In controls, neuropil staining was usually lighter than in the cell bodies of pyramidal cells (not shown in higher magnification, but see Fig. 4C,F).

In the white matter between the subiculum and the EC, fibers of probable glial and axonal origin (Fig. 7K, left) stained positively for mGluR5. These fibers seem to arise from the border of the EC gray matter, invading the white matter toward the subicular complex and the hippocampus (see excerpts in Fig. 7J,K). Interstitial neurons in the white matter (Fig. 7K, right, hash signs) were also strongly IR to mGluR5. None of these profiles were detectable in non-HS or control hippocampi.

Analysis of Covariance and Effects of AEDs or Other Psychoactive Drugs

Given the differences in neuronal densities, GFAP (Fig. 1), and MAP2 expression (Fig. 3), an important question was whether the statistical differences in mGluR5 expression for the three groups could be accounted for by changes in neuronal densities, astrogliosis, or MAP2 expression. We therefore performed an analysis of covariance (ANCOVA) comparing groups and neuronal densities, GFAP, and MAP2 IR area with mGluR5 IR area and the results are shown in Table 2. Difference between groups in mGluR5 IR remained significant in all subfields after cell count, GFAP, and MAP2 correction (Table 2, boldfaced values). These results indicate that the three patient categories showed significant differences in mGluR5 expression levels that were not influenced by changes in neuronal densities, MAP2 expression, or GFAP. Nevertheless, we have confirmed with confocal microscopy of merged images (mGluR5 and GFAP staining) that astroglial elements colocalized with considerable amount of mGluR5 positive fibers in the HS DG (Fig. 8).

All epileptic patients were taking antiepileptic drugs (AEDs) either as monotherapy or polytherapy (up to four concomitant AEDs) at time of surgery: carbamazepine (65%), clobazam, or phenobarbital (30%), and phenytoin (20%). No patient was taking topiramate. Two patients were also taking antidepressant (fluoxetine). There were no differences in averaged mGluR5, MAP2 expression, neuronal densities, GFAP, or neo-Timm staining between patients taking a given AED as compared to those not taking that drug (unpaired t tests; $P > 0.27$).

Epilepsy Duration, Seizure Frequency, and Febrile Seizures

In the HS group there was no correlation between duration of epilepsy before surgery, seizure frequency, or age at surgery

FIGURE 7. mGluR5 immunohistochemical expression in human hippocampal formation: Ammon's horn, subicular complex, and entorhinal cortex. In HS CA4 (A, left), mGluR5 was upregulated in pyramidal neurons. In control CA4 (A, right) mGluR5 staining was light and predominant in the neuropil. HS CA3 (B) staining pattern exhibited few immunopositive fibers and neurons. On the other hand, HS CA2 (C, left) showed densely stained pyramidal neurons and packed tortuous dendrites in the radiatum-lacunosum. Arrowheads in CA2 point to interneurons. Non-HS CA2 (C, right) exhibited dense neuropil staining with visible long and organized dendrites, a typical pattern in all non-HS Ammon's horn subfields. In the stratum oriens margin between CA2 and CA1, interneurons were also strongly mGluR5 positive in HS cases (D, left), but not in non-HS (D, right). In the Sommer's sector, HS CA1 (E, left) and prosubiculum (F) exhibited mGluR5 staining in the few remaining neurons (asterisks) and a mesh of strongly mGluR5 positive fibers. Subiculum (G) showed dense immunostaining in the neuropil and in transverse neuronal fibers. The cytoplasm of pyramidal cells was less strong IR than the neuropil. Nuclei and blood vessels were devoid of immunoreactivity. A similar pattern was observed in the islands of parasubiculum (H) and in the presubiculum (I), where primary dendrites showed distinctive strong IR. A similar staining pattern was found in non-HS cases. The entorhinal cortex (J) also displayed marked neuropil staining (J, left), which was also a feature of non-HS cases. In HS, EC layer II clusters of neurons (J, right) from where perforant path fibers arise were especially stained. In the white matter enclosed between the subiculum and the entorhinal cortex (K, left), numerous fibers of probable glial and axonal origin were positively stained. Such fibers seem to emerge from the entorhinal cortex in direction to the subicular complex and hippocampus (J and K, excerpts). Strong mGluR5 immunoreactivity was also found in interstitial white matter neurons (K right, hash signs). Such profiles were not distinguishable in non-HS or in control hippocampal formation. [Color figure can be viewed in the online issue, which is available at wileyonlinelibrary.com.]

TABLE 2.

Analysis of Covariance (ANCOVA) Comparing Patients' Categories (Group) and Neuronal Density (Counts), MAP2 IR Area (MAP2) or GFAP IR (GFAP) Area With mGluR5 IR Area (mGluR5)

Subfield		mGluR5 (counts as covariable)	mGluR5 (MAP2 as covariable)	mGluR5 (GFAP as covariable)
Granular layer				
	Group	**11.569/0.000**	**13.889/0.000**	**16.506/0.000**
Hilus				
	Group	**9.102/0.001**	**7.828/0.002**	**6.270/0.005**
CA4				
	Group	**38.556/0.000**	**30.156/0.000**	**21.799/0.000**
CA3				
	Group	**25.280/0.000**	**17.564/0.000**	**12.881/0.000**
CA2				
	Group	**47.267/0.000**	**25.063/0.000**	**33.825/0.000**
CA1				
	Group	**355.359/0.000**	**288.500/0.000**	**315.094/0.000**
Prosubiculum				
	Group	**205.597/0.000**	**146.848/0.000**	**153.799/0.000**
Subiculum				
	Group	**34.141/0.000**	**37.135/0.000**	**44.749/0.000**
Parasubiculum				
	Group	**28.646/0.000**	**24.805/0.000**	**31.359/0.000**
Entorhinal cortex				
	Group	**14.096/0.000**	**17.521/0.000**	**31.754/0.000**

Data are presented as *F*-values/*P*-values, and significant results are indicated in boldfaced type.

with mGluR5 expression. However, in the non-HS group we found a strong negative correlation between GL mGluR5 expression and seizure frequency (Fig. 5K; $R = -0.91$, $P = 0.004$), and between CA2 mGluR5 expression and epilepsy duration (Fig. 5L; $R = -0.79$, $P = 0.03$).

In the HS group, we analyzed mGluR5 differences in FS-negative specimens as compared to other FS-positive specimens. History of FS was identified in 10 of 35 patients, negative in 16 patients and unknown in 9 patients (therefore such unclear cases were not considered for statistical analyses). The only sector that differed in mGluR5 expression was CA2: it was almost twice the value in FS-negative specimens as compared to FS-positive specimens (no-FS: 139327 ± 45002 μm^2 *versus* FS: 79001 ± 24479 μm^2; $P = 0.015$). FS-negative specimens also exhibited 1.15-fold increase in MAP2 IR area in CA2 (no-FS: 29656 ± 3614 μm^2 versus FS: 25748 ± 1765 μm^2; $P = 0.015$) and 1.22-fold increase in the entorhinal cortex (no-FS: 27018 ± 4552 μm^2 versus FS: 22137 ± 3985 μm^2; $P = 0.015$). There were no differences in neuronal counts, neo-Timm staining, or GFAP expression between the two groups.

DISCUSSION

In this study, we described and quantified mGluR5 abnormalities across the hippocampal formation of HS and non-HS patients with pharmacoresistant TLE and of non-epileptic controls. We correlated mGluR5 expression with classical neuropathological hallmarks of HS and further evaluated mGluR5 differences related to previous occurrence of an initial precipitating injury such as febrile seizures. As with any human study, assumptions in experimental design and methodology must be considered when interpreting our results. For instance, it

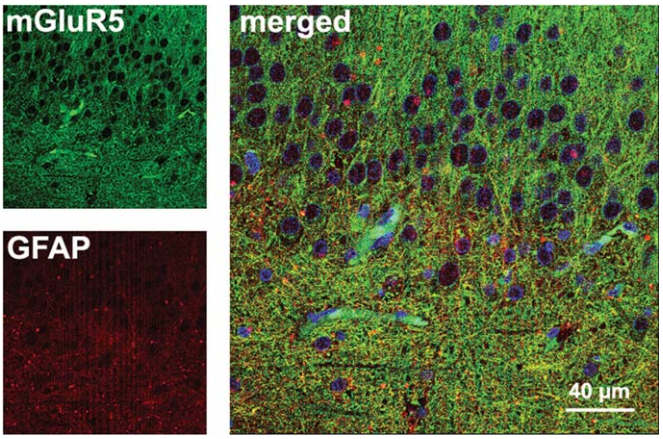

FIGURE 8. Double-labeled immunofluorescence in the HS dentate gyrus. In the hilus, yellow astrocytic fibers were seen in the merged image of GFAP (red) and mGluR5 (green). Nuclei of granule cells and other cell types appeared in blue (Hoechst staining). [Color figure can be viewed in the online issue, which is available at wileyonlinelibrary.com.]

should be understood that mGluR5 immunoreactivity does not necessarily equal functional activity; however, in this discussion we will assume, based on evidences in the literature and in our correlation data, that such a relationship exists in some circumstances. Despite this assumption, our results show differences between HS and non-HS patients that can be compared and contrasted with other human and animal studies and suggest several hypotheses related to hippocampal function in TLE patients. It is worth reemphasizing that this was a retrospective study from a single epilepsy center where patients were approved for surgery based on the diagnosis that the seizure onsets were in the temporal lobe, and the *en bloc* surgical resection was designed to remove the focus for pathologic examination. The strengths of this approach are that the patients were uniformly medically evaluated, and the independent statistical variables, such as the pathogenic categories and IPI histories, were not the primary consideration for surgery. However, our results may not be as relevant to patients with unilateral extratemporal or bilateral hemispheric seizures, and may represent only some of the possible pathophysiological associations and/or mechanisms. Such strategy has been used by our group and others (Babb et al., 1984b, 1991; Mathern et al., 1995a,b, 1999; Proper et al., 2000; Leite et al., 2002; Notenboom et al., 2006; Kandratavicius et al., 2012; Peixoto-Santos et al., 2012).

We found a very typical mGluR5-staining pattern in TLE specimens, with highest immunoreactivity in the EC (up to 21-fold increase in mGluR5 IR area as compared to control specimens) and in the subiculum (sevenfold increase), sectors not investigated in previous studies (Tang et al., 2001; Notenboom et al., 2006). Previous studies describing mGluR5 upregulation in surgical TLE hippocampi have speculated that this phenomenon could contribute to hyperexcitability (Tang et al., 2001; Notenboom et al., 2006). In fact, there is neurophysiological evidence that group I mGluRs play synergistic effects in induction of prolonged bursts of interictal activity in disinhibited rat hippocampal slices, but not in the maintenance of ictal discharges (Merlin, 2002). Group I mGluRs second messenger pathways are mainly coupled to phospholipase C/calcium cascade (Gerber et al., 2007), and activation of such pathways results in intracellular calcium store release (Kawabata et al., 1996). Calcium levels determine their action as facilitators or depressors of *N*-methyl-D-aspartate (NMDA) receptor responses (Harney et al., 2006) and thus modulate synaptic plasticity. In cultured hippocampal neurons, group I mGluR activation is associated with internalization of synaptic NMDA and non-NMDA receptors, modulating long-term depression (LTD) (Snyder et al., 2001). In addition to regulation of LTD and long-term potentiation (LTP), group I mGluRs might also control glutamate release (Rodriguez-Moreno et al., 1998).

Human hippocampal mGluR5 expression levels before epilepsy onset and before seizures become intractable are unknown. However in TLE animal models, mGluR5 downregulation following *status epilepticus* (Akbar et al., 1996; Kirschstein et al., 2007) gives place to chronic astrocytic mGluR5 upregulation (Aronica et al., 2000; Ulas et al., 2000). This might be associated with spread of neuron-glia calcium waves and release of glial glutamate, modulating synaptic transmission and neuronal excitability (Vermeiren et al., 2005; Ding et al., 2007). In the present study, inverse correlation between GFAP and mGluR5 expression seen in controls was lost in HS specimens and was strongly positive in non-HS. One hypothesis is that deficient glutamate uptake could be one underlying factor leading to increased mGluR5 expression in astrocytes across the epileptogenic hippocampal formation, that is, in HS cases. The OML receives strong excitatory inputs from perforant path axons originated in the EC and in some cases from sprouted mossy fibers, resulting in excessive glutamate levels. In the DG and especially in the DG-ML, decreased glial glutamate transporter has been found in HS hippocampi (Mathern et al., 1999), which contributes to enhance excitation (Rothstein et al., 1996). Despite excessive extracellular glutamate, mGluR5 overexpression could lead to temporary desensitization of glutamate excitatory responses by internalization of ionotropic glutamate receptors (Snyder et al., 2001) and inhibition of glutamate release (Rodriguez-Moreno et al., 1998), resulting in counterbalance of a hyperexcitable system.

The EC plays a pivotal role in bidirectional connection of the hippocampus with the neocortex while the DG acts as a hippocampal gate, filtering excitatory signals from the EC (Hsu, 2007). The EC can generate epileptiform discharges and seizures, as demonstrated in ictal intracranial EEG recordings by Spencer and Spencer (1994). Patients might exhibit seizures originating from the EC alone, from the hippocampus alone or both. The proportion of these seizure types might be influenced by the degree of hippocampal pathology/cell loss and the reorganization that occurs within the different hippocampal formation subfields. In the present study, HS specimens had significant neuronal loss in the EC, similar to the pattern described by others (Cavanagh and Meyer, 1956; Falconer et al., 1964; Du et al., 1993). Neurons from EC layer III project directly to the subiculum and CA1-CA3 (Yeckel and Berger, 1990), and connections between the subicular complex and EC are extensive and reciprocal (Amaral et al., 1984; Hevner and Kinney, 1996). Strong neuropil mGluR5 immunoreactivity in HS EC is likely a result of upregulation in dendritic, axonal, and glial compartments. Inasmuch as EC lesions might lead to hippocampal hyperexcitability, this process is facilitated by loss of excitatory drive from the subicular complex to the EC (Schwarcz et al., 2000). In our series, we did not observe pyramidal cell loss in subiculum and parasubiculum of MTLE cases, suggesting that connectivity between the subicular complex and EC is preserved, and seizures initiated within the EC would spread to the hippocampus. Interestingly, in vitro studies have shown that EC ictal discharges may be abolished by interictal CA3-CA1 activity/low frequency stimulation when Schaffer collaterals are not impaired (Barbarosie and Avoli, 1997). Thus, mGluR5-mediated LTD induction within CA3-CA1 subfields would help in disruption of reverberant circuit EC-subiculum-Ammon's horn, controlling the emergence of spontaneous recurrent seizures.

The subiculum exhibits enhanced hyperexcitability (Knopp et al., 2005; Wozny et al., 2005), being capable to synchronize

epileptiform discharges between CA3 and EC in disinhibited rat slices (Benini and Avoli, 2005). In a recent study, Huberfeld et al. (2011) demonstrated a pivotal role for the subiculum in the transition between interictal and ictal activity, both in slices from mesial temporal resections and in intracranial EEG recording. Subicular neurons generate recurrent pre-ictal discharges emerging from interictal activity of much lower amplitude. Interictal discharges at the same recording sites were preceded by interneuron firing and dependent of both glutamatergic and depolarizing GABAergic transmission. In contrast, pre-ictal discharges were dependent on glutamatergic mechanisms, preceded by pyramidal cells firing and occurring for long duration (median 25 min) before a seizure occurs, which suggests that synaptic plasticity mechanisms are necessary. In this context, we might speculate a potential contribution for mGluR5 in the modulation of NMDA-dependent synaptic mechanisms involved in the transition from pre-ictal to ictal events in the subiculum. Another possibility would be its central role in NMDA-independent plasticity mechanisms involved during this phenomenon.

In cultures of pyramidal hippocampal neurons, the application of group I mGluR agonists can switch the cells into a "neuroprotective mode", protecting them against NMDA-induced toxicity (Bruno et al., 2001). The protective mode would be favored by local high extracellular glutamate, as also seen in cerebellar cultures (Pizzi et al., 1996). Protection is null with previous mGluR5 inhibition, indicating that activation of mGluR5 is largely required for induction of the switch in response to group I mGluR agonism (Bruno et al., 2001). Subicular mGluR5 overexpression as seen in hippocampal specimens of the present study could effectively contribute to a protective mode and survival of local pyramidal cells. Indeed we did not, like others, observe cell loss in the subicular complex. However, as in other areas discussed above, there might be considerable influence of astrogliosis in subiculum mGluR5 immunoreactivity.

In CA2, we found strong mGluR5 and MAP2 immunoreactivity in sclerotic HS hippocampi. Although strong mGluR5 immunoreactivity in HS CA2 had already been shown in illustrations from Tang et al. (2001), their study could not further discuss its significance as they did not have a control group. We have determined that mGluR5 immunoreactivity in HS CA2 is 2.4-fold the value of controls and in this context, it is reasonable to speculate that mGluR5 could be involved in known protective mechanisms that naturally spare CA2 from the massive damage seen in classical HS. More specifically, local mGluR5 could be involved in adaptive mechanisms that would allow pyramidal cells to survive. Indeed, mGluR5 IR pattern in HS CA2 was similar to the calcium-binding protein parvalbumin staining described in monkeys (Leranth and Ribak, 1991) and in HS hippocampi (Sloviter et al., 1991). Calcium overload may lead to excitotoxic cell damage, at what increased expression of calcium-binding proteins and calcium chelation are neuroprotective (Scharfman and Schwartzkroin, 1989). Whereas CA2 can generate independent epileptiform activity (Wittner et al., 2009), activation of mGluR5 in presence of low or no calcium depresses NMDA-mediated synaptic transmission (Harney et al., 2006), suggesting a protective role as similarly described by Baskys et al. (2005). The presence of inhibitory basket and chandelier interneurons would also help depress the firing rate of CA2 pyramidal cells (Leranth and Ribak, 1991).

In our HS specimens, interneurons were also strongly mGluR5-positive. Recent in vitro studies with rat hippocampal slices have shown that mGluR5 activation during seizures may contribute to selective interneurons death in CA1 alveus-oriens (Sanon et al., 2010). By contrast, there is evidence of long-lasting depression of glutamatergic excitation in CA1 interneurons upon mGluR5 activation especially at the stratum radiatum (Le Duigou et al., 2011), which may be protective.

Stimulation-induced LTD is dependent on mGluR5 activation (Harney et al., 2006). Repeated LTD in the hippocampus might lead to reduction of synaptic strength and persistent decrease in synaptic structures (Shinoda et al., 2005). Loss of mGluR5-dependent LTD during initial phases of epileptogenesis (Kirschstein et al., 2007), i.e., before establishment of chronic seizures and seizure intractability, could impair elimination of aberrant glutamatergic synapses in the DG, thus contributing to the development of mossy fiber sprouting. In our series, we found a positive correlation between OML mGluR5 immunoreactivity and mossy fiber sprouting in HS hippocampi. Therefore, in DG from chronic drug-resistant MTLE, upregulated mGluR5 could arise as an adaptive mechanism counterbalancing excessive hyperexcitability and aborting mossy fiber sprouting progression.

In addition, we found increased MAP2 IR area in cell bodies and dendritic processes in the HS granular layer, CA2, and subicular complex. MAP2 is a compulsory protein participating in neurite outgrowth (Caceres et al., 1992). HS granular layer dendritic MAP2 expression increases within the same time window in which mossy fiber sprouting occurs in the kainate animal model (Pollard et al., 1994). In human MTLE, granular cell dendrites in contact with mossy fiber aberrant collaterals exhibit increased spine density (Isokawa, 1997, 2000). Although some studies have shown diminished pyramidal dendritic spines in human MTLE (Scheibel et al., 1974) and in pilocarpine model (Kurz et al., 2008), a net increase in dendritic branching has been demonstrated in different controlled animal experiments (Kato et al., 2001; Arisi and Garcia-Cairasco, 2007). Altogether, these studies suggest that induction and maintenance of axonal sprouting is frequently accompanied by dendritic sprouting, regardless of possible changes in spine density. Neuronal MAP2 phosphorylation is regulated by metabotropic and NMDA glutamate receptors in a bidirectional fashion: while mGluR activation results in increased MAP2 phosphorylation, NMDA induces a sustained decrease (Quinlan and Halpain, 1996). Dendrite protein synthesis is particularly dependent on group I mGluRs activation in the hippocampus (Gong et al., 2006). Thus overexpressed mGluR5 in dendrites of MTLE hippocampi possibly plays an important role in this form of synaptic plasticity, as also suggested by our results of positive correlation between mGluR5 and MAP2 expression in CA3 and in CA1 in HS specimens.

Studies have speculated that HS may arise from progressive injury from intractable seizures (Meldrum and Corsellis, 1984; Sloviter, 1994). There are also theories on developmental etiology underlying HS (Blumcke et al., 2002) or alternatively, an initial insult triggering later development of HS and MTLE (Gastaut et al., 1959; Falconer and Taylor, 1968; Mathern et al., 1995b). Ten of our HS specimens were derived from MTLE patients with previous history of FS during childhood. Although FS is associated with increased risk for epilepsy and HS (Cendes et al., 1993), molecular mechanisms that mediate a possible link between FS with HS and later seizures remain unclear (McClelland et al., 2011). We posed the question of whether differences in mGluR5 immunoreactivity would be found between FS-positive and FS-negative specimens. We acknowledge that our groups were small, but yet, no evaluation of mGluR5 immunoreactivity has ever been described in human MTLE hippocampi regarding FS. We also recognize that these results reflect decades after a FS occurred and thus speculation of mGluR5 status before and after the insult in view of present findings cannot be easily supported. Our results indicate that FS-negative specimens had almost twice the values of CA2 mGluR5 and CA2 MAP2 immunoreactivities, as compared to FS-positive specimens. CA2 and CA3 receive the major hypothalamic projections to the hippocampal formation (Ballmaier et al., 2008), with the hippocampus acting as modulator of neuroendocrine neurons within this axis (Herman et al., 1989). Secretion of hypothalamic-pituitary-adrenal axis hormones is decreased during fever, with reduced cortisol levels being pro-epileptogenic (Perez-Cruz et al., 2007). Reduced baseline levels of mGluR5 in these sectors at time of the injury could be associated with decreased compensatory mechanisms to molecular changes related to toxicity. This could be related not only to susceptibility for symptomatic seizures during acute febrile illnesses, but also to facilitation of epileptogenesis development.

In our series, non-HS cases showed a variable degree of hippocampal neuronal loss, astrogliosis and mossy fiber sprouting, demonstrating that such cases actually display slightly abnormal hippocampi. As stressed by Proper et al. (2000), an important point of consideration in these cases is, not only to remove the temporal cortex, but also to include resection of the hippocampus. Non-HS group exhibited increased mGluR5 expression in the hilus, CA4-1, and prosubiculum when compared to HS, and our correlation analysis suggest that different mechanisms underlie the distinct morphological changes. For instance, increased seizure frequency correlated with decreased mGluR5 expression only in non-HS cases. It is noteworthy that in a hippocampus that is not the major ictal source and that is better preserved than an HS specimen, mGluR5 is also overexpressed and the more mGlur5, the less seizures were observed. In other words, a protective role for mGluR5 seems feasible, especially in non-HS cases.

The topic whether is the agonism or the antagonism of mGluR5 neuroprotective is controversial. For instance, studies have shown group I mGluRs agonist-induced neuroprotection in slices of 7-day-old rats (Blaabjerg et al., 2003), while antagonism of group I mGluRs conferred neuroprotection in 14 days mice mixed cultures (Bruno et al., 2000). There is evidence that the different and unknown mechanisms that underlie controversial results between species may operate via mechanisms other than through the mGluR5 receptor (Lea et al., 2005). Likewise, pro- and antiepileptogenic mechanisms mGluR5-related may differ considerably depending on age, species, and brain region. Activation of group I mGluRs in disinhibited rat hippocampal slices result in ictal discharges (Merlin, 2002) and seizures in young mice after intracerebroventricular agonist injection (Chapman et al., 2000). Intracerebroventricular group I mGluRs antagonist injection has anticonvulsant effect in young rats, but not in adults (Lojkova and Mares, 2005). Absence of anticonvulsant effect of the specific mGluR5 negative allosteric modulator 2-Methyl-6-(phenylethynyl)pyridine (MPEP) in adult rats was also seen in the pentylenetetrazole (PTZ) model (Mares, 2009), although a protective effect against LTP induction was accomplished when MPEP was injected before lower doses of PTZ (Nagaraja et al., 2005). This latter study points to the concept that mGluR5 activation might be required to seizure initiation, but not to the maintenance of ictal discharges (Merlin, 2002). However, seizures can be triggered in the mGluR5 knockout mouse (Witkin et al., 2008). An age-specific mGluR5 expression profile could partly explain the lack of anticonvulsant effect of group I mGluRs antagonists in the adult rat (Lojkova and Mares, 2005; Mares, 2009), since a decline in mGluR5 expression occurs after the peak during the second postnatal week (Romano et al., 1996). In MTLE animal models, acute mGluR5 downregulation in CA1 after pilocarpine-induced *status epilepticus* (Kirschstein et al., 2007) and chronic upregulation in the DG and CA1 in the kindling model have been demonstrated (Akbar et al., 1996). It is not known if isolated provoked seizures without induction of *status epilepticus* could change mGluR5 expression. Animal studies covering acute, latent, and chronic phases of epileptogenesis would better help understanding mGluR5 expression changes as causative or compensatory factors in epileptogenesis.

In summary, our findings suggest that mGluR5 upregulation also participates in counterbalance mechanisms along the hyperexcitable circuitry uniquely altered in TLE hippocampal formation. We have described differential mGluR5 upregulation in HS and non-HS, with identification of maximum abnormalities involving previously unevaluated EC and subicular complex, and in the usually preserved CA2 sector. We have further determined the correlation between mGluR5 with mossy fiber sprouting and Ammon's horn dendritic abnormalities, which are pathological landmarks of recurrent reverberant hyperexcitability exclusive to HS. Inefficient post-synaptic compensatory morphological (dendritic branching) and molecular (mGluR5 expression) mechanisms at CA2 sector could underlie the association of FS with HS and epilepsy. Whereas mGluR5 is an excitatory group I mGluR that could well contribute to a pro-excitatory net state, our results also support a co-existing rather protective role for this receptor in TLE. Further studies evaluating receptor functional states and expression of other

interacting proteins could provide additional insights for its role in epileptogenesis and seizure intractability.

Acknowledgments

Part of this study has been presented as a poster in the 64th Annual Meeting of the American Epilepsy Society (San Antonio, TX, USA, Dec 2010). We thank Renata Caldo Scandiuzzi and Jose Eduardo Peixoto-Santos for the excellent technical support in neo-Timm histochemistry and confocal immunofluorescence. The authors declare that they have no conflict of interest. The funders had no role in study design, data collection and analysis, decision to publish, or preparation of the manuscript.

REFERENCES

Abercrombie M. 1946. Estimation of nuclear population from microtome sections. Anat Rec 94:239–247.

Akbar MT, Rattray M, Powell JF, Meldrum BS. 1996. Altered expression of group I metabotropic glutamate receptors in the hippocampus of amygdala-kindled rats. Brain Res Mol Brain Res 43:105–116.

Amaral DG, Insausti R, Cowan WM. 1984. The commissural connections of the monkey hippocampal formation. J Comp Neurol 224: 307–336.

Arisi GM, Garcia-Cairasco N. 2007. Doublecortin-positive newly born granule cells of hippocampus have abnormal apical dendritic morphology in the pilocarpine model of temporal lobe epilepsy. Brain Res 1165:126–134.

Aronica E, van Vliet EA, Mayboroda OA, Troost D, da Silva FH, Gorter JA. 2000. Upregulation of metabotropic glutamate receptor subtype mGluR3 and mGluR5 in reactive astrocytes in a rat model of mesial temporal lobe epilepsy. Eur J Neurosci 12:2333–2344.

Babb TL, Brown WJ, Pretorius J, Davenport C, Lieb JP, Crandall PH. 1984a. Temporal lobe volumetric cell densities in temporal lobe epilepsy. Epilepsia 25:729–740.

Babb TL, Kupfer WR, Pretorius JK, Crandall PH, Levesque MF. 1991. Synaptic reorganization by mossy fibers in human epileptic fascia dentata. Neuroscience 42:351–363.

Babb TL, Lieb JP, Brown WJ, Pretorius J, Crandall PH. 1984b. Distribution of pyramidal cell density and hyperexcitability in the epileptic human hippocampal formation. Epilepsia 25:721–728.

Ballmaier M, Narr KL, Toga AW, Elderkin-Thompson V, Thompson PM, Hamilton L, Haroon E, Pham D, Heinz A, Kumar A. 2008. Hippocampal morphology and distinguishing late-onset from early-onset elderly depression. Am J Psychiatry 165:229–237.

Barbarosie M, Avoli M. 1997. CA3-driven hippocampal-entorhinal loop controls rather than sustains in vitro limbic seizures. J Neurosci 17:9308–9314.

Baskys A, Fang L, Bayazitov I. 2005. Activation of neuroprotective pathways by metabotropic group I glutamate receptors: A potential target for drug discovery? Ann NY Acad Sci 1053:55–73.

Benini R, Avoli M. 2005. Rat subicular networks gate hippocampal output activity in an in vitro model of limbic seizures. J Physiol 566:885–900.

Berg AT. 2009. Identification of pharmacoresistant epilepsy. Neurol Clin 27:1003–1013.

Blaabjerg M, Fang L, Zimmer J, Baskys A. 2003. Neuroprotection against NMDA excitotoxicity by group I metabotropic glutamate receptors is associated with reduction of NMDA stimulated currents. Exp Neurol 183:573–580.

Blumcke I, Becker AJ, Klein C, Scheiwe C, Lie AA, Beck H, Waha A, Friedl MG, Kuhn R, Emson P, et al. 2000. Temporal lobe epilepsy associated up-regulation of metabotropic glutamate receptors: correlated changes in mGluR1 mRNA and protein expression in experimental animals and human patients. J Neuropathol Exp Neurol 59:1–10.

Blumcke I, Coras R, Miyata H, Ozkara C. 2012. Defining clinico-neuropathological subtypes of mesial temporal lobe epilepsy with hippocampal sclerosis. Brain Pathol 22:402–411.

Blumcke I, Thom M, Wiestler OD. 2002. Ammon's horn sclerosis: A maldevelopmental disorder associated with temporal lobe epilepsy. Brain Pathol 12:199–211.

Bruno V, Battaglia G, Copani A, Cespedes VM, Galindo MF, Cena V, Sanchez-Prieto J, Gasparini F, Kuhn R, Flor PJ, et al. 2001. An activity-dependent switch from facilitation to inhibition in the control of excitotoxicity by group I metabotropic glutamate receptors. Eur J Neurosci 13(8):1469–1478.

Bruno V, Ksiazek I, Battaglia G, Lukic S, Leonhardt T, Sauer D, Gasparini F, Kuhn R, Nicoletti F, Flor PJ. 2000. Selective blockade of metabotropic glutamate receptor subtype 5 is neuroprotective. Neuropharmacology 39:2223–2230.

Caceres A, Mautino J, Kosik KS. 1992. Suppression of MAP2 in cultured cerebellar macroneurons inhibits minor neurite formation. Neuron 9:607–618.

Cavanagh JB, Meyer A. 1956. Aetiological aspects of Ammon's horn sclerosis associated with temporal lobe epilepsy. Br Med J 2:1403–1407.

Cendes F, Andermann F, Dubeau F, Gloor P, Evans A, Jones-Gotman M, Olivier A, Andermann E, Robitaille Y, Lopes-Cendes I, et al. 1993. Early childhood prolonged febrile convulsions, atrophy and sclerosis of mesial structures, and temporal lobe epilepsy: An MRI volumetric study. Neurology 43:1083–1087.

Chapman AG, Nanan K, Williams M, Meldrum BS. 2000. Anticonvulsant activity of two metabotropic glutamate group I antagonists selective for the mGlu5 receptor: 2-methyl-6-(phenylethynyl)-pyridine (MPEP), and (E)-6-methyl-2-styryl-pyridine (SIB 1893). Neuropharmacology 39:1567–1574.

Ding S, Fellin T, Zhu Y, Lee SY, Auberson YP, Meaney DF, Coulter DA, Carmignoto G, Haydon PG. 2007. Enhanced astrocytic Ca2+ signals contribute to neuronal excitotoxicity after status epilepticus. J Neurosci 27:10674–10684.

Du F, Whetsell WO Jr, Abou-Khalil B, Blumenkopf B, Lothman EW, Schwarcz R. 1993. Preferential neuronal loss in layer III of the entorhinal cortex in patients with temporal lobe epilepsy. Epilepsy Res 16:223–233.

Engel J Jr. 1996. Surgery for seizures. N Engl J Med 334:647–652.

Engel J Jr. 2001. Mesial temporal lobe epilepsy: What have we learned? Neuroscientist 7:340–352.

Falconer MA, Serafetinides EA, Corsellis JA. 1964. Etiology and pathogenesis of temporal lobe epilepsy. Arch Neurol 10:233–248.

Falconer MA, Taylor DC. 1968. Surgical treatment of drug-resistant epilepsy due to mesial temporal sclerosis. Etiology and significance. Arch Neurol 19:353–361.

Gastaut H, Toga M, Roger J, Gibson WC. 1959. A correlation of clinical electroencephalographic and anatomical findings in nine autopsied cases of 'temporal lobe epilepsy'. Epilepsia 1:56–85.

Gerber U, Gee CE, Benquet P. 2007. Metabotropic glutamate receptors: Intracellular signaling pathways. Curr Opin Pharmacol 7:56–61.

Gittins R, Harrison PJ. 2004. Neuronal density, size and shape in the human anterior cingulate cortex: A comparison of Nissl and NeuN staining. Brain Res Bull 63:155–160.

Gong R, Park CS, Abbassi NR, Tang SJ. 2006. Roles of glutamate receptors and the mammalian target of rapamycin (mTOR) signaling pathway in activity-dependent dendritic protein synthesis in hippocampal neurons. J Biol Chem 281:18802–18815.

Harney SC, Rowan M, Anwyl R. 2006. Long-term depression of NMDA receptor-mediated synaptic transmission is dependent on activation of metabotropic glutamate receptors and is altered to long-term potentiation by low intracellular calcium buffering. J Neurosci 26:1128–1132.

Herman JP, Schafer MK, Young EA, Thompson R, Douglass J, Akil H, Watson SJ. 1989. Evidence for hippocampal regulation of neuroendocrine neurons of the hypothalamo-pituitary-adrenocortical axis. J Neurosci 9:3072–3082.

Hevner RF, Kinney HC. 1996. Reciprocal entorhinal-hippocampal connections established by human fetal midgestation. J Comp Neurol 372:384–394.

Hsu D. 2007. The dentate gyrus as a filter or gate: A look back and a look ahead. In: Scharfman HE, editor. Progress in Brain Research. Amsterdam: Elsevier. pp 601–613.

Huberfeld G, Menendez de la Prida L, Pallud J, Cohen I, Le Van Quyen M, Adam C, Clemenceau S, Baulac M, Miles R. 2011. Glutamatergic pre-ictal discharges emerge at the transition to seizure in human epilepsy. Nat Neurosci 14:627–634.

Isokawa M. 1997. Preservation of dendrites with the presence of reorganized mossy fiber collaterals in hippocampal dentate granule cells in patients with temporal lobe epilepsy. Brain Res 744:339–343.

Isokawa M. 2000. Remodeling dendritic spines of dentate granule cells in temporal lobe epilepsy patients and the rat pilocarpine model. Epilepsia 41(Suppl 6):S14–S17.

Kandratavicius L, Hallak JE, Young LT, Assirati JA, Carlotti CG Jr, Leite JP. 2012. Differential aberrant sprouting in temporal lobe epilepsy with psychiatric co-morbidities. Psychiatry Res 195:144–150.

Kato K, Masa T, Tawara Y, Kobayashi K, Oka T, Okabe A, Shiosaka S. 2001. Dendritic aberrations in the hippocampal granular layer and the amygdalohippocampal area following kindled-seizures. Brain Res 901:281–295.

Kawabata S, Tsutsumi R, Kohara A, Yamaguchi T, Nakanishi S, Okada M. 1996. Control of calcium oscillations by phosphorylation of metabotropic glutamate receptors. Nature 383:89–92.

Kirschstein T, Bauer M, Muller L, Ruschenschmidt C, Reitze M, Becker AJ, Schoch S, Beck H. 2007. Loss of metabotropic glutamate receptor-dependent long-term depression via downregulation of mGluR5 after status epilepticus. J Neurosci 27:7696–7704.

Knopp A, Kivi A, Wozny C, Heinemann U, Behr J. 2005. Cellular and network properties of the subiculum in the pilocarpine model of temporal lobe epilepsy. J Comp Neurol 483:476–488.

Kurz JE, Moore BJ, Henderson SC, Campbell JN, Churn SB. 2008. A cellular mechanism for dendritic spine loss in the pilocarpine model of status epilepticus. Epilepsia 49:1696–1710.

Le Duigou C, Holden T, Kullmann DM. 2011. Short- and long-term depression at glutamatergic synapses on hippocampal interneurons by group I mGluR activation. Neuropharmacology 60:748–756.

Lea PMt, Movsesyan VA, Faden AI. 2005. Neuroprotective activity of the mGluR5 antagonists MPEP and MTEP against acute excitotoxicity differs and does not reflect actions at mGluR5 receptors. Br J Pharmacol 145:527–534.

Leite JP, Chimelli L, Terra-Bustamante VC, Costa ET, Assirati JA, de Nucci G, Martins AR. 2002. Loss and sprouting of nitric oxide synthase neurons in the human epileptic hippocampus. Epilepsia 43(Suppl 5):235–242.

Leranth C, Ribak CE. 1991. Calcium-binding proteins are concentrated in the CA2 field of the monkey hippocampus: A possible key to this region's resistance to epileptic damage. Exp Brain Res 85:129–136.

Lojkova D, Mares P. 2005. Anticonvulsant action of an antagonist of metabotropic glutamate receptors mGluR5 MPEP in immature rats. Neuropharmacology 49(Suppl 1):219–229.

Lorente de No R. 1934. Studies on the structure of the cerebral cortex II. Continuation of study of the ammonic system. J Psychol Neurol 46:113–177.

Mares P. 2009. Age-dependent anticonvulsant action of antagonists of group I glutamate metabotropic receptors in rats. Epilepsy Res 83:215–223.

Mathern GW, Adelson PD, Cahan LD, Leite JP. 2002. Hippocampal neuron damage in human epilepsy: Meyer's hypothesis revisited. Prog Brain Res 135:237–251.

Mathern GW, Babb TL, Pretorius JK, Leite JP. 1995a. Reactive synaptogenesis and neuron densities for neuropeptide Y, somatostatin, and glutamate decarboxylase immunoreactivity in the epileptogenic human fascia dentata. J Neurosci 15:3990–4004.

Mathern GW, Babb TL, Vickrey BG, Melendez M, Pretorius JK. 1995b. The clinical-pathogenic mechanisms of hippocampal neuron loss and surgical outcomes in temporal lobe epilepsy. Brain 118(Pt 1):105–118.

Mathern GW, Mendoza D, Lozada A, Pretorius JK, Dehnes Y, Danbolt NC, Nelson N, Leite JP, Chimelli L, Born DE, et al. 1999. Hippocampal GABA and glutamate transporter immunoreactivity in patients with temporal lobe epilepsy. Neurology 52:453–472.

McClelland S, Dube CM, Yang J, Baram TZ. 2011. Epileptogenesis after prolonged febrile seizures: mechanisms, biomarkers and therapeutic opportunities. Neurosci Lett 497:155–162.

Meldrum BS, Corsellis JAN. 1984. Epilepsy. In: Adams JH, Corsellis JAN, Duchen LW, editors. Greenfield's Neuropathology, 4th ed. London: Edward Arnold. pp 921–950.

Merlin LR. 2002. Differential roles for mGluR1 and mGluR5 in the persistent prolongation of epileptiform bursts. J Neurophysiol 87: 621–625.

Nagaraja RY, Becker A, Reymann KG, Balschun D. 2005. Repeated administration of group I mGluR antagonists prevents seizure-induced long-term aberrations in hippocampal synaptic plasticity. Neuropharmacology 49(Suppl 1):179–187.

Notenboom RG, Hampson DR, Jansen GH, van Rijen PC, van Veelen CW, van Nieuwenhuizen O, de Graan PN. 2006. Up-regulation of hippocampal metabotropic glutamate receptor 5 in temporal lobe epilepsy patients. Brain 129:96–107.

Peixoto-Santos JE, Galvis-Alonso OY, Velasco TR, Kandratavicius L, Assirati JA, Carlotti CG, Jr., Scandiuzzi RC, Serafini LN, Leite JP. 2012. Increased metallothionein I/II expression in patients with temporal lobe epilepsy. Plos One 7:11.

Perez-Cruz C, Lonsdale D, Burnham WM. 2007. Anticonvulsant actions of deoxycorticosterone. Brain Res 1145:81–89.

Pizzi M, Galli P, Consolandi O, Arrighi V, Memo M, Spano PF. 1996. Metabotropic and ionotropic transducers of glutamate signal inversely control cytoplasmic Ca2+ concentration and excitotoxicity in cultured cerebellar granule cells: pivotal role of protein kinase C. Mol Pharmacol 49:586–594.

Pollard H, Khrestchatisky M, Moreau J, Ben-Ari Y, Represa A. 1994. Correlation between reactive sprouting and microtubule protein expression in epileptic hippocampus. Neuroscience 61:773–787.

Proper EA, Oestreicher AB, Jansen GH, Veelen CW, van Rijen PC, Gispen WH, de Graan PN. 2000. Immunohistochemical characterization of mossy fibre sprouting in the hippocampus of patients with pharmaco-resistant temporal lobe epilepsy. Brain 123:19–30.

Quinlan EM, Halpain S. 1996. Postsynaptic mechanisms for bidirectional control of MAP2 phosphorylation by glutamate receptors. Neuron 16:357–368.

Rodriguez-Moreno A, Sistiaga A, Lerma J, Sanchez-Prieto J. 1998. Switch from facilitation to inhibition of excitatory synaptic transmission by group I mGluR desensitization. Neuron 21:1477–1486.

Romano C, van den Pol AN, O'Malley KL. 1996. Enhanced early developmental expression of the metabotropic glutamate receptor mGluR5 in rat brain: Protein, mRNA splice variants, and regional distribution. J Comp Neurol 367:403–412.

Rothstein JD, Dykes-Hoberg M, Pardo CA, Bristol LA, Jin L, Kuncl RW, Kanai Y, Hediger MA, Wang Y, Schielke JP, et al. 1996. Knockout of glutamate transporters reveals a major role for astroglial transport in excitotoxicity and clearance of glutamate. Neuron 16:675–686.

Sanon NT, Pelletier JG, Carmant L, Lacaille JC. 2010. Interneuron subtype specific activation of mGluR1/5 during epileptiform activity in hippocampus. Epilepsia 51:1607–1618.

Scharfman HE, Schwartzkroin PA. 1989. Protection of dentate hilar cells from prolonged stimulation by intracellular calcium chelation. Science 246:257–260.

Scheibel ME, Crandall PH, Scheibel AB. 1974. The hippocampal-dentate complex in temporal lobe epilepsy. A Golgi study. Epilepsia 15:55–80.

Schwarcz R, Eid T, Du F. 2000. Neurons in layer III of the entorhinal cortex. A role in epileptogenesis and epilepsy? Ann NY Acad Sci 911:328–342.

Shinoda Y, Kamikubo Y, Egashira Y, Tominaga-Yoshino K, Ogura A. 2005. Repetition of mGluR-dependent LTD causes slowly developing persistent reduction in synaptic strength accompanied by synapse elimination. Brain Res 1042:99–107.

Sloviter RS. 1994. The functional organization of the hippocampal dentate gyrus and its relevance to the pathogenesis of temporal lobe epilepsy. Ann Neurol 35:640–654.

Sloviter RS, Sollas AL, Barbaro NM, Laxer KD. 1991. Calcium-binding protein (calbindin-D28K) and parvalbumin immunocytochemistry in the normal and epileptic human hippocampus. J Comp Neurol 308:381–396.

Snyder EM, Philpot BD, Huber KM, Dong X, Fallon JR, Bear MF. 2001. Internalization of ionotropic glutamate receptors in response to mGluR activation. Nat Neurosci 4:1079–1085.

Spencer SS, Spencer DD. 1994. Entorhinal-hippocampal interactions in medial temporal lobe epilepsy. Epilepsia 35:721–727.

Stan AD, Ghose S, Gao XM, Roberts RC, Lewis-Amezcua K, Hatanpaa KJ, Tamminga CA. 2006. Human postmortem tissue: What quality markers matter? Brain Res 1123:1–11.

Tang FR, Lee WL, Yeo TT. 2001. Expression of the group I metabotropic glutamate receptor in the hippocampus of patients with mesial temporal lobe epilepsy. J Neurocytol 30:403–411.

Ulas J, Satou T, Ivins KJ, Kesslak JP, Cotman CW, Balazs R. 2000. Expression of metabotropic glutamate receptor 5 is increased in astrocytes after kainate-induced epileptic seizures. Glia 30:352–361.

Vermeiren C, Najimi M, Vanhoutte N, Tilleux S, de Hemptinne I, Maloteaux JM, Hermans E. 2005. Acute up-regulation of glutamate uptake mediated by mGluR5a in reactive astrocytes. J Neurochem 94:405–416.

Witkin JM, Baez M, Yu J, Eiler WJ II. 2008. mGlu5 receptor deletion does not confer seizure protection to mice. Life Sci 83:377–380.

Wittner L, Huberfeld G, Clemenceau S, Eross L, Dezamis E, Entz L, Ulbert I, Baulac M, Freund TF, Magloczky Z, et al. 2009. The epileptic human hippocampal cornu ammonis 2 region generates spontaneous interictal-like activity in vitro. Brain 132:3032–3046.

Wozny C, Knopp A, Lehmann TN, Heinemann U, Behr J. 2005. The subiculum: A potential site of ictogenesis in human temporal lobe epilepsy. Epilepsia 46(Suppl 5):17–21.

Yeckel MF, Berger TW. 1990. Feedforward excitation of the hippocampus by afferents from the entorhinal cortex: Redefinition of the role of the trisynaptic pathway. Proc Natl Acad Sci USA 87:5832–5836.